Table B.1 COD Load Estimates of Tributaries

(kg/year)

		Burnot p.	Eger viz	Tapolca p.	Keki p.	Fuzfoi sed	Orvenyesi sed	Nemesvitai a.	Jamai p.	Tetves p.	Zala
1994											
M1	Monit data	121619.7	116182.3	126117.1	6070.3	10726.6	10905.2	126682	29302.5	36995.6	9881475
M2	CODmean*V	116207.3	128952.8	99766.6	8111.7	8579.7	17336.1	155208	47841.7	58811.7	10775325
M3	Load=f*(Q)	116358.5	144844.1	116345.9	21382.5	11571.0	13974.7	121731	42066.1	91924.5	10113135
	Discharge, m3	5679303	4768965	7029622	935963	429812	1588716	2359891	2296401	4277217	266034240
	M3/M1	0.96	1.25	0.92	3.52	1.08	1.28	0.96	1.44	2.48	1.02
1995											
M1	Monit data	114199.6	123450.4	228905.5	8050.9	15871.3	37015.5	182360	37572.9	233964.7	10898569
M2	COD mean*V	123625.6	131663.8	155889.8	11068.1	15402.8	26644.9	265878	48174.7	131620.7	11126287
M3	Load=f*(Q)	126138.4	155017.6	145553.5	35500.4	20077.0	28068.5	254393	51647.4	352787.5	11261116
	Discharge, m3	6506610	5155511	8444029	1141946	713093	1877724	4881941	2669116	6837438	301471200
	M3/M1	1.10	1.26	0.64	4.41	1.26	0.76	1.40	1.37	1.51	1.03

M1,M2,M3 mean different calculation methods (refer to section 2.1 for details)

Table B.2 TN Load Estimates of Tributaries

(kg/year)

		Burnot p.	Eger viz	Tapolca p.	Keki p.	Fuzfoi sed	Orvenyesi sed	Nemesvitai a.	Jamai p.	Tetves p.	Zala
1994											
M1	Monit data	38863.5	28600.3	66004.6	6021.1	3545.9	10007.1	8557.4	1952.5	10748.5	920636
M2	TNmean*V	29440.7	22781.5	52383.8	8039.1	2217.9	16644.4	6970.8	2884.9	11598.4	947761
M3	Load=f*(Q)	31970.1	34825.4	56135.8	13368.3	2507.5	12037.9	7856.8	3728.1	22978.6	856599
	Discharge, m3	5679303	4768965	7029622	935963	429812	1588716	2359891	2296401	4277217	266034240
	M3/M1	0.82	1.22	0.85	2.22	0.71	1.20	0.92	1.91	2.14	0.93
1995											
M1	Monit data	24661.4	26892.1	86221.5	6778.3	2310.0	14256.9	9732.8	3262.2	36091.8	837424
M2	TNmean*V	24602.5	24607.7	62560.5	10270.5	2684.2	38597.4	11754.2	5164.7	28586.2	794173
M3	Load=f*(Q)	34772.4	35884.7	67430.6	19938.0	4375.5	14069.4	15550.4	4414.7	45146.0	912017
	Discharge, m3	6506610	5155511	8444029	1141946	713093	1877724	4881941	2669116	6837438	301471200
	M3/M1	1.41	1.33	0.78	2.94	1.89	0.99	1.60	1.35	1.25	1.09

M1,M2,M3 mean different calculation methods (refer to section 2.1 for details)

Table B.3 TP Load Estimates of Tributaries

(kg/year)

		Burnot p.	Eger viz	Tapolca p.	Keki p.	Fuzfoi sed	Orvenyesi sed	Nemesvitai a.	Jamai p.	Tetves p.	Zala
1994											
M1	Monit. data	672.2	626	3699.9	98.3	121.5	74.6	660.4	132.4	262.5	40231
M2	TP mean*V	607.7	1553.0	3582.3	133.4	104.7	80.7	826	230.6	595.2	48459
M3	Load=f*(Q)	714.1	756.2	3255.5	233.5	96.2	103.4	576.5	190.2	1579.5	39299
	Discharge, m3	5679303	4768965	7029622	935963	429812	1588716	2359891	2296401	4277217	266034240
	M1/M3	1.06	1.21	0.88	2.38	0.79	1.39	0.87	1.44	6.02	0.98
1995											
M1	Monit data	616	618.4	3781.4	107.3	112.8	238.4	439.2	173.8	3905.7	41490
M2	TP mean*V	696.2	755.0	2754.1	148.4	117.1	218.5	821.7	204.2	1618.1	51784
M3	Load=f*(Q)	653.0	751.4	3543.0	359.7	166.6	168.2	837.8	221.0	6663.4	42811
	Discharge, m3	6506610	5155511	8444029	1141946	713093	1877724	4881941	2669116	6837438	301471200
	M1/M3	1.06	1.22	0.94	3.35	1.48	0.71	1.91	1.27	1.71	1.03

M1,M2,M3 mean different calculation methods (refer to section 2.1 for details)

Table B.4 Runoffs from Keszthely Residential Area in 1997

Watershed: Budos arok, 280 ha

Date	UnitTP load kg/y/ha	UnitTN load kg/y/ha	UnitCOD load kg/y/ha	Rain mm	Runoff rate
17-Jun	4.83	66.2	609.5	10	0.30
3-Nov	2.91	52.6	207.5	27	0.31

Table B.5 Runoffs from Fonyod Residential Area in 1997

Site: Fonyod Varhegy North Watershed area: 38.08 ha (32.08 ha urban, 6 ha forest and park)
Calculation with runoff coefficients assumed by DDT KOFE

Date	Rain, mm mm	Rain intensity mm/h	Runoff rate	TP kg kg	Unit TP load kg/ha/year	TN kg	Unit TN load kg/ha/year	COD kg	Unit COD load kg/ha/year
14-Jun	10	4	0.25	0.69	1.27	3.24	5.96	32.4	59.56
23-Jun	9.3	4.2	0.25	0.53	1.05	3.96	7.83	27.4	54.16
6-Jul	17	7.8	0.25	1.24	1.34	2.78	3.01	36.5	39.47
13-Nov	32.2	1.84	0.085	0.55	0.31	3.42	1.95	16.4	9.36
Averages					0.99		4.69		40.64

Table B.6 Corrected Runoffs from Fonyod Residential Area in 1997

Calculation with runoff coefficient calculated from discharge data of the experiments in the Keszthely urban area

Date	Rain, mm mm	Rain intensity mm/h	Runoff rate	TP kg kg	Unit TP load kg/ha/year	TN kg	Unit TN load kg/ha/year	COD kg	Unit COD load kg/ha/year
14-Jun	10	4	0.31	0.86	1.57	4.02	7.39	40.2	73.85
23-Jun	9.3	4.2	0.31	0.66	1.30	4.91	9.71	34.0	67.16
6-Jul	17	7.8	0.31	1.54	1.66	3.45	3.73	45.3	48.94
13-Nov	32.2	1.84	0.31	0.68	0.39	4.24	2.42	20.3	11.61
Averages					1.23		5.81		50.39

Table B.7 Correlation Coefficients for Basin Characteristics of Sub-catchments (n=50)

		A	A^1/2	P/A	S	Omat	Sero	Omat*Sero	C+T	Rec	C+T+Rec	Ara	Pas	For	Vin	Ara+Vin	W
Catchment area (A)	ha	1.0000															
Average flow path (A^1/2)	km	0.9538	1.0000														
Population dencity (P/A)	person/ha	-0.2280	-0.3040	1.0000													
Ratio of area more than 3deg. Slope (S)	%	-0.1676	-0.1440	-0.1983	1.0000												
Average organic matter contents (Omat)	%	-0.2690	-0.3355	0.3953	-0.2336	1.0000											
Average of soil erosion possibility (Sero)	-	0.1458	0.1481	-0.2519	0.3534	-0.4999	1.0000										
Omat*Sero	-	0.0703	0.0608	-0.1453	0.3990	-0.0056	0.7860	1.0000									
City and Town area (C+T)	%	-0.1749	-0.2366	0.7604	-0.1349	0.2417	-0.2898	-0.2507	1.0000								
Recreational area (Rec)	%	-0.2207	-0.3085	0.5878	-0.2075	0.4528	-0.2968	-0.1352	0.2379	1.0000							
City and Town + Recreational area (C+T+Rec)	%	-0.2534	-0.3507	0.8047	-0.2252	0.4682	-0.3648	-0.2185	0.6308	0.9037	1.0000						
Arable land (Ara)	%	0.4090	0.5171	-0.3154	-0.2029	-0.0223	-0.0678	0.0725	-0.2483	-0.3394	-0.3806	1.0000					
Pasture (Pas)	%	-0.0163	-0.0219	-0.1697	-0.1337	0.3070	0.0918	0.2659	-0.0881	-0.2451	-0.2346	-0.0417	1.0000				
Forest (For)	%	0.1051	0.1619	-0.4116	0.4837	-0.3741	0.0789	0.0333	-0.2595	-0.4276	-0.4559	-0.1907	-0.0827	1.0000			
Vineyard (Vin)	%	-0.2217	-0.2712	-0.0646	0.1202	-0.4057	0.4789	0.0673	-0.1599	-0.1728	-0.2085	-0.3471	-0.1642	-0.2277	1.0000		
Arable land + Vineyard (Ara+Vin)	%	0.2160	0.2802	-0.3507	-0.0991	-0.3383	0.3096	0.1216	-0.3613	-0.4580	-0.5251	0.6804	-0.1680	-0.3594	0.4511	1.0000	
Wetland and Water body (W)	%	-0.1569	-0.2123	0.0394	-0.3017	0.2026	-0.1795	-0.2324	0.0194	0.2422	0.2020	-0.1888	-0.1391	-0.4914	0.3267	0.0756	1.0000

Table B.8 Data for the Analysis of the Relation between Runoff Load and Land Characteristics

Name of river(shed)	Population Density	Average length	Slope ratio (>3deg.)	Average organic matter contents	Soil erosion posibility	City, Town and Recreational area
	perso/ha	km	%	t/ha	%	%
	P	L	S	O	E	T
Fuzfoi sed	1.90	3.08	0.439	249	20.6	28.6
Keki patak	2.42	2.91	0.607	183	5.4	12.6
Orvenyesi sed	0.34	5.07	0.560	140	28.3	2.1
Burnot patak	0.25	9.09	0.457	151	51.3	3.3
Eger patak	0.34	19.01	0.412	187	43.4	2.4
Tapolca patak	3.86	6.70	0.177	204	35.7	10.0
Tetves patak	0.36	8.53	0.502	165	21.0	2.4
Jamai patak	0.89	7.05	0.344	183	21.0	7.2

	1994				1995			
Name of river(shed)	Discharge (m3/km2/y)	COD (kg/km2/y)	T-N (kg/km2/y)	T-P (kg/km2/y)	Discharge (m3/km2/y)	COD (kg/km2/y)	T-N (kg/km2/y)	T-P (kg/km2/y)
Fuzfoi sed	45387	1222	265	10.2	75300	2120	462	17.6
Keki patak	110373	2522	1576	27.5	134663	4186	2351	42.4
Orvenyesi sed	61842	544	469	4.0	73092	1093	548	6.5
Burnot patak	68740	1408	387	8.6	78753	1527	421	7.9
Eger patak	13202	401	96	2.1	14272	429	99	2.1
Tapolca patak	156457	2589	1249	72.5	187937	3240	1501	78.9
Tetves patak	58793	1264	316	21.7	93985	4849	621	91.6
Jamai patak	46168	846	75	3.8	53661	1038	89	4.4

Table B.9 Correlation Coefficients for Multiple Regression Analysis

	P	L	S	E	T
Population density (P):person/ha	1.0000				
Average length of the basin (L):km2	-0.4448	1.0000			
Ratio of area more than 3deg. slope (S):%	-0.4953	-0.2145	1.0000		
Average of soil erosion possibility (E):%	-0.2967	0.6469	-0.4039	1.0000	
Ratio of residential and recreational area (T):%	0.5324	-0.5512	-0.0791	-0.4283	1.0000
Discharge94 : m3/ha/year	0.8225	-0.4938	-0.3324		0.0331
COD94 : kg/ha/year	0.8322	-0.4931	-0.2027	-0.5313	0.2740
T-N94 : kg/ha/year	0.7576	-0.4705	0.0368	-0.6218	0.1218
T-P94 : kg/ha/year	0.8591	-0.2466	-0.5678	-0.3654	0.0928
Discharge95 : m3/ha/year	0.8338	-0.5558	-0.2982		0.2077
COD95 : kg/ha/year	0.4242	-0.4385	0.1604	-0.5473	0.1457
T-N95 : kg/ha/year	0.7105	-0.5043	0.1567	-0.5080	0.2146
T-P95 : kg/ha/year	0.4750	-0.2091	-0.2050	-0.2785	-0.0148

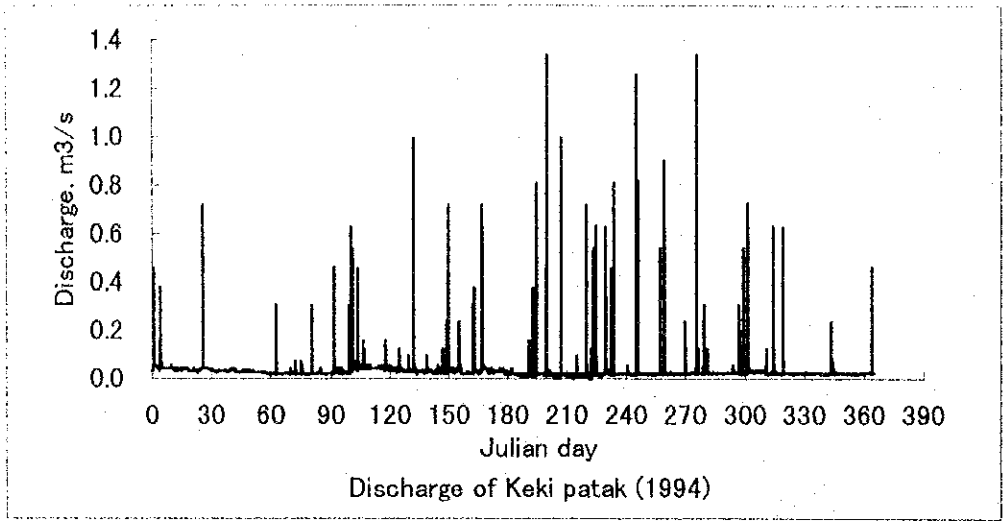

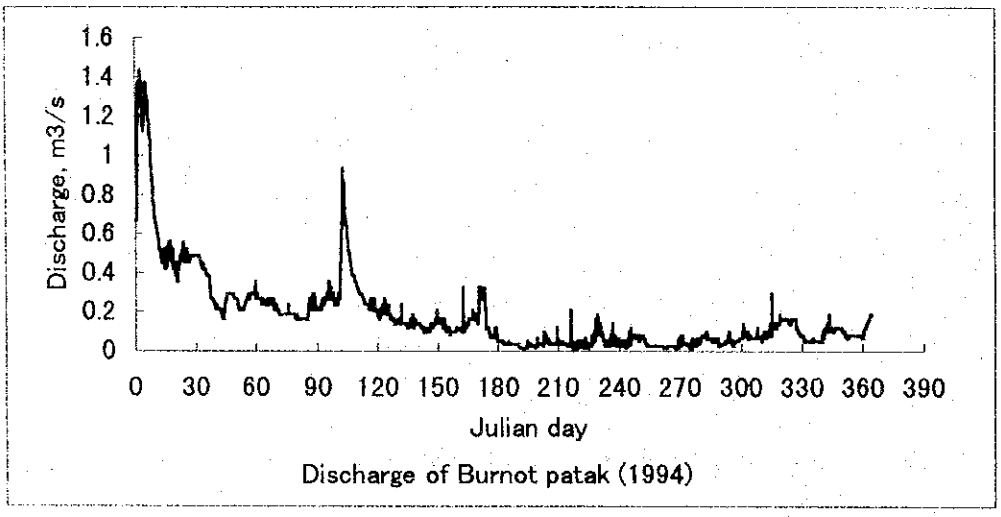

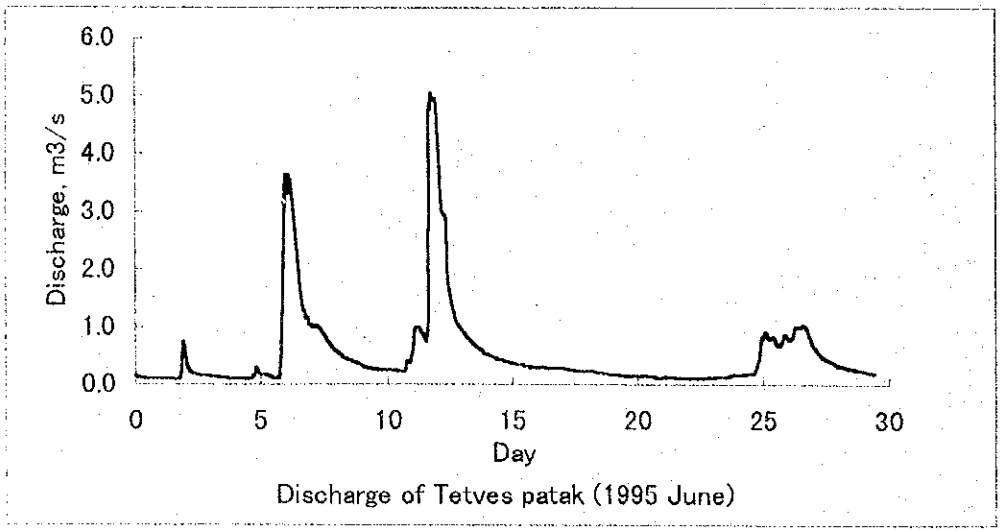

Figure B.1 Annual Discharges of Kéki Patak, Burnót Patak, and Tetves Patak

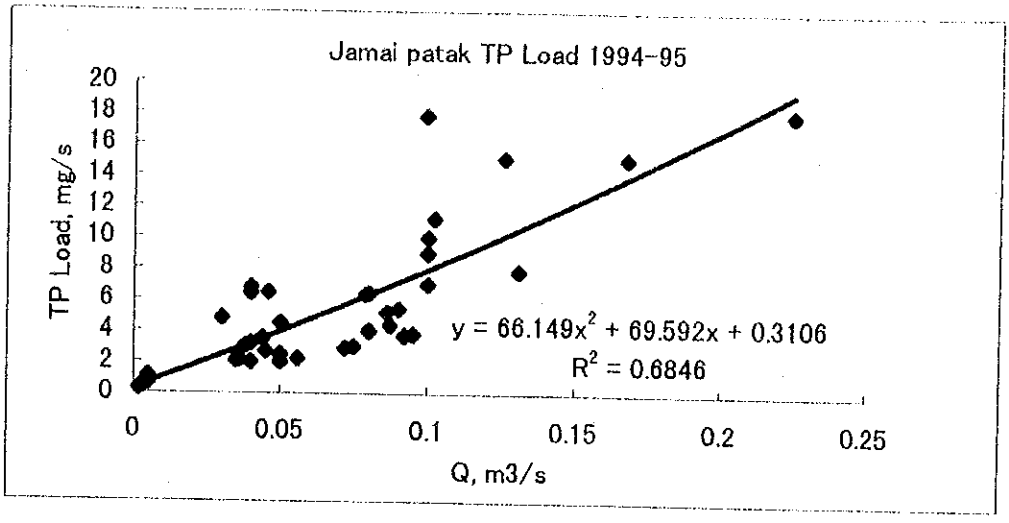

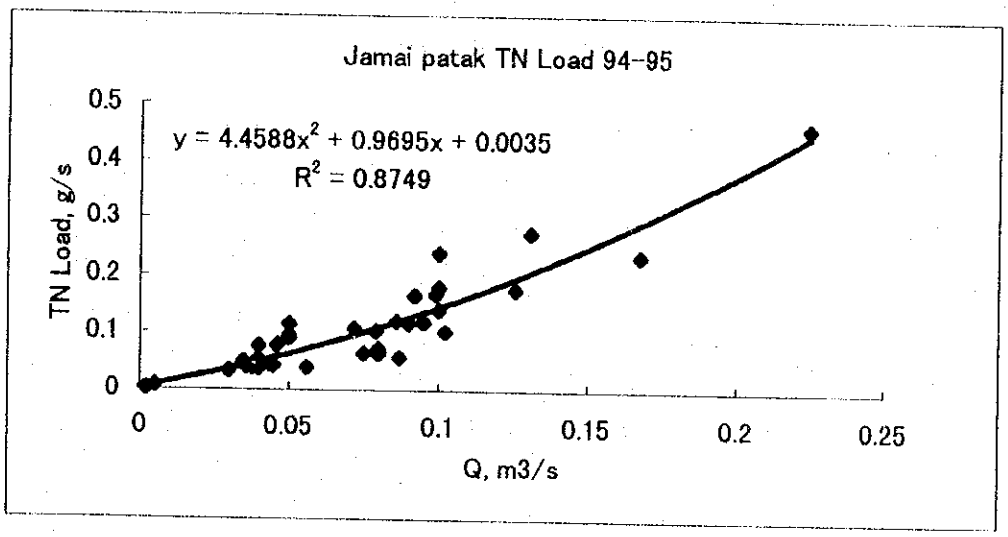

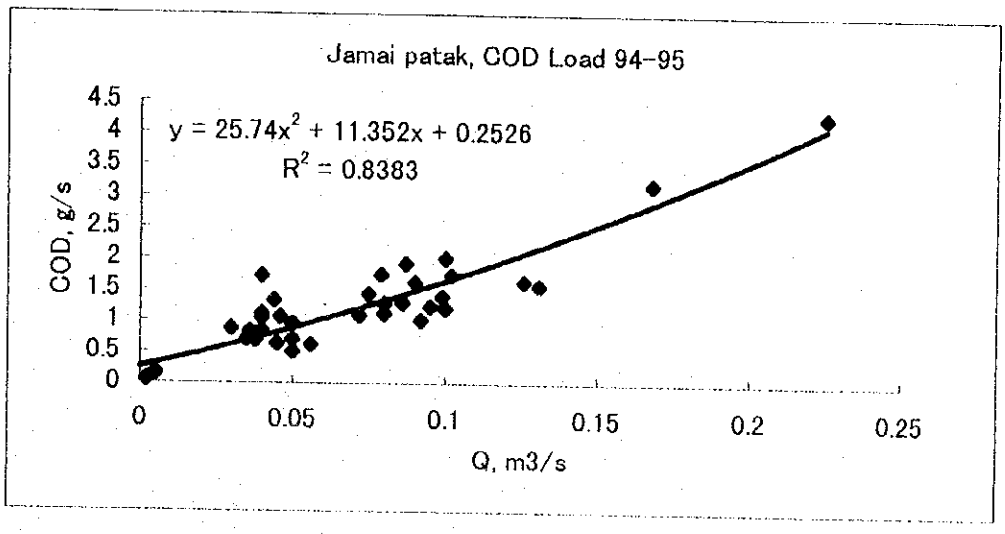

Figure B.2 Best Fit Curve for Load-discharge Correlations (Jamai)

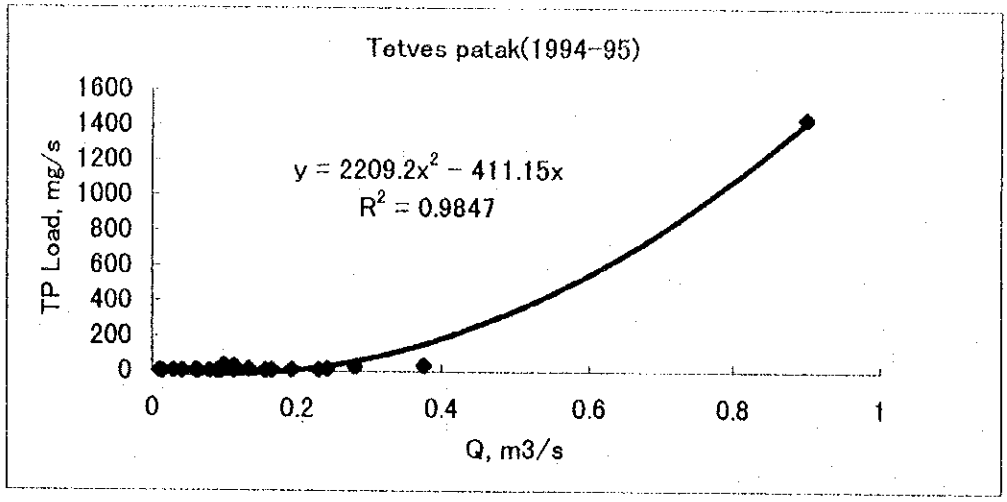

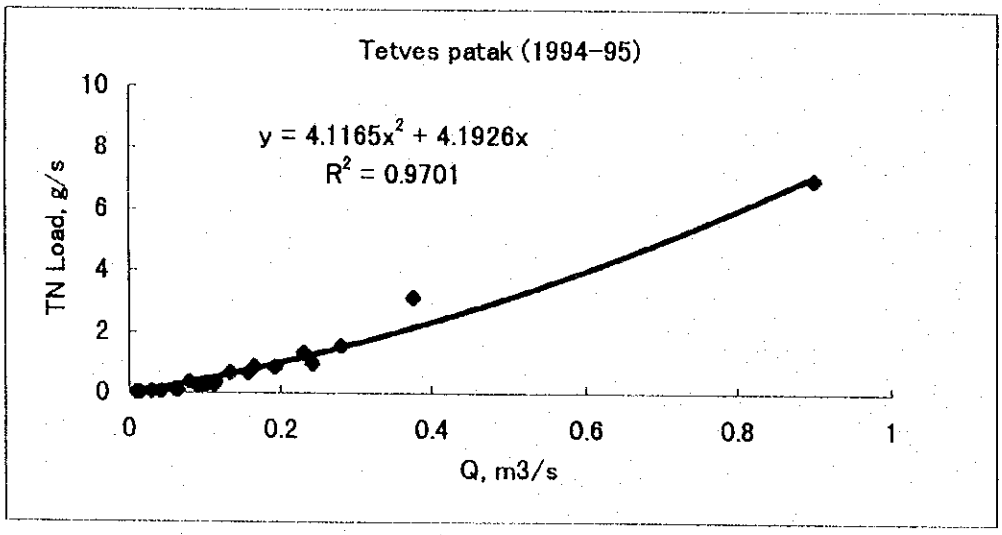

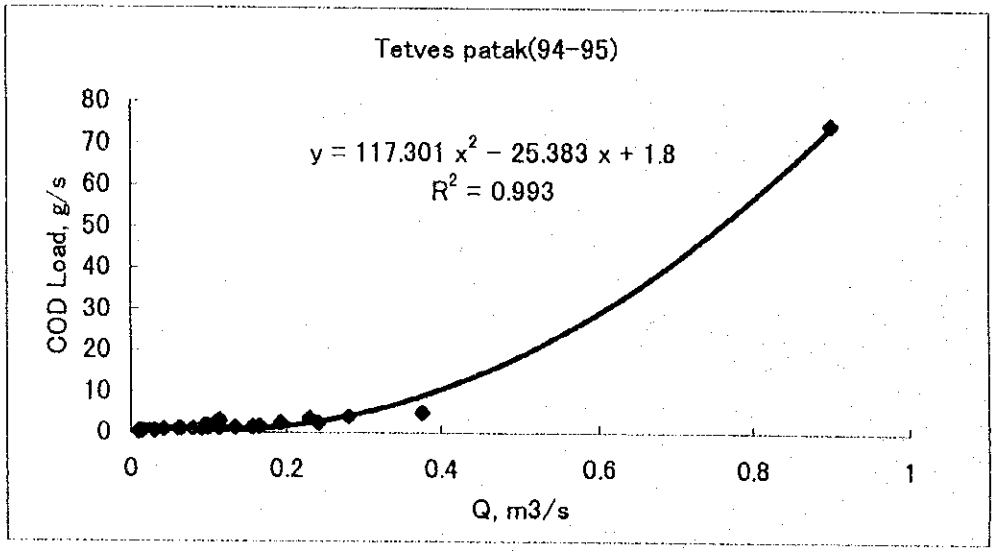

Figure B.3 Best Fit Curve for Load-discharge Correlations (Tetves Patak)

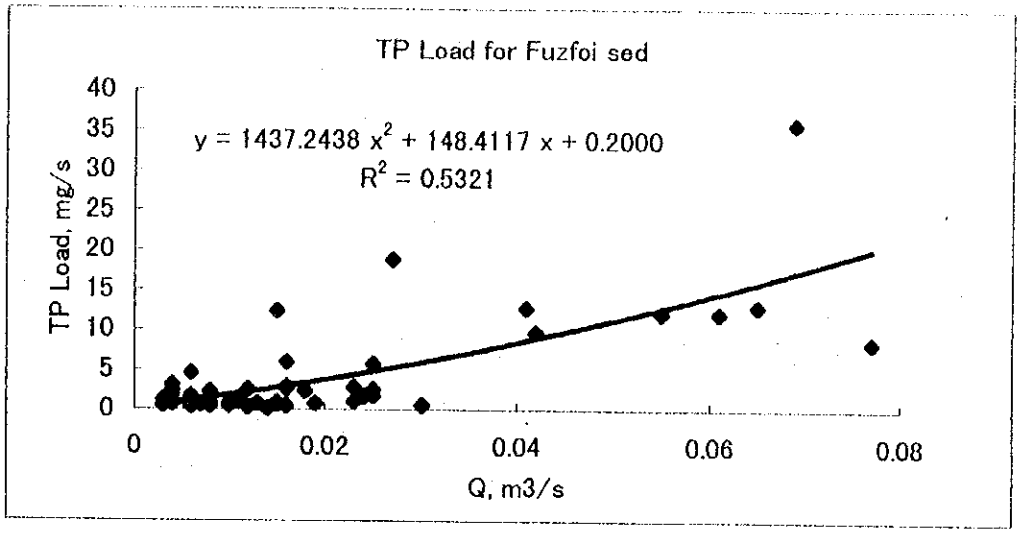

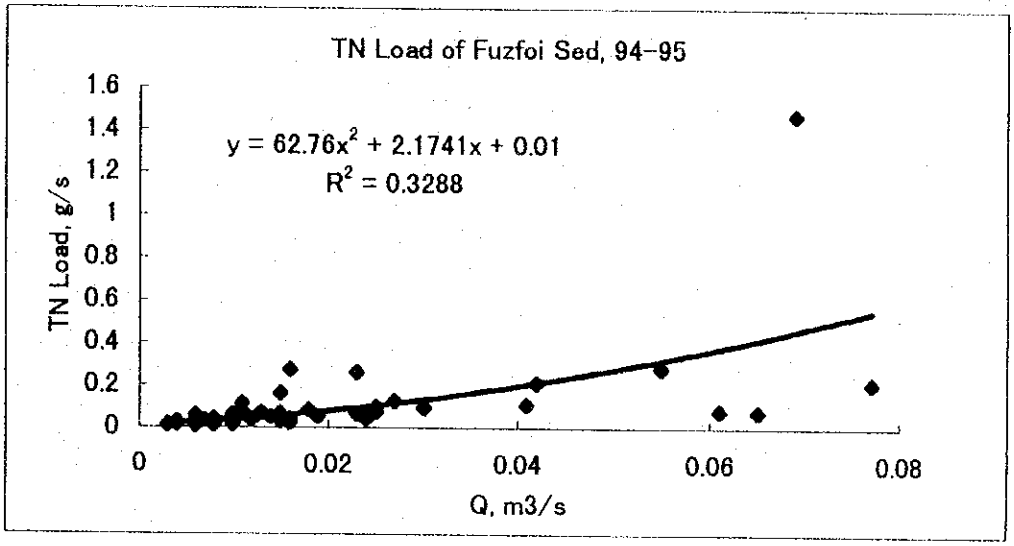

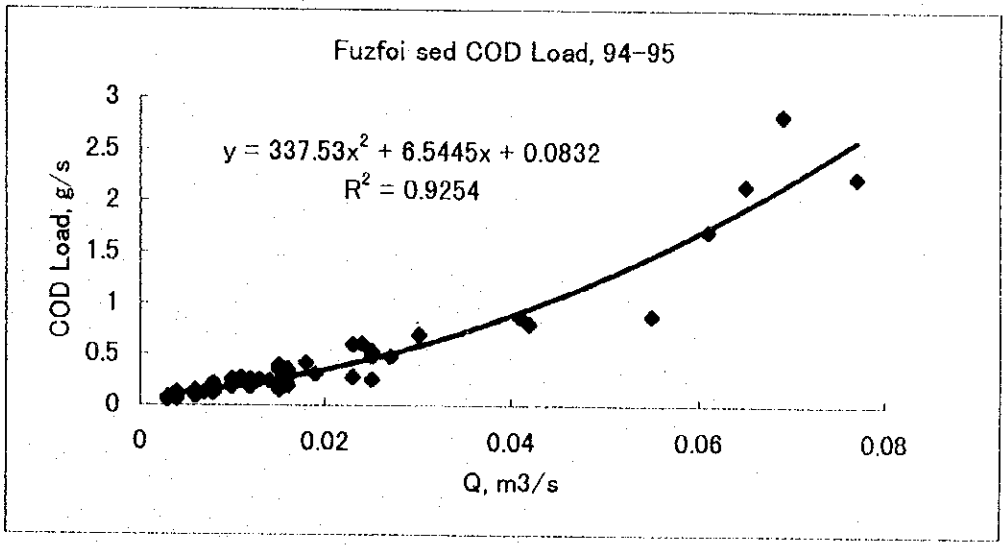

Figure B.4 Best Fit Curve for Load-discharge Correlations (Fuzfoi)

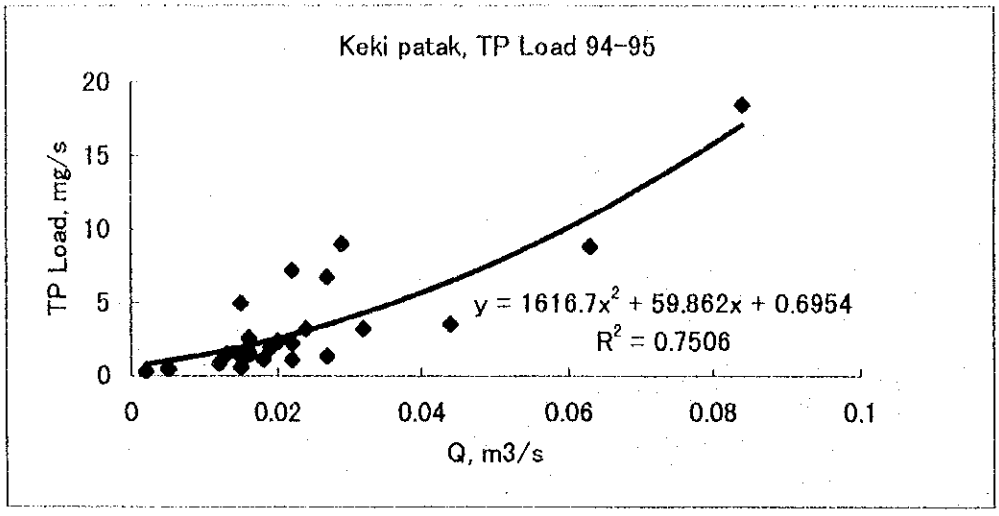

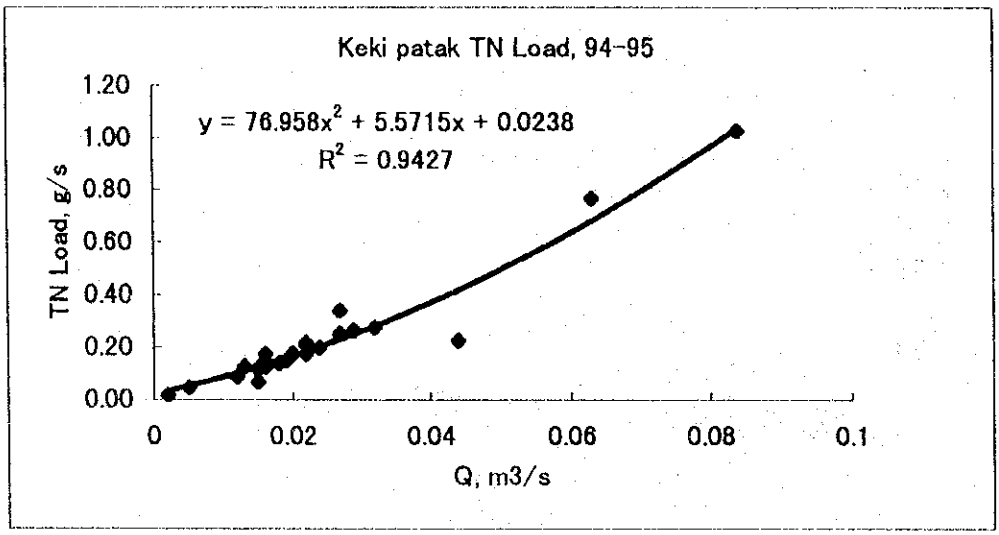

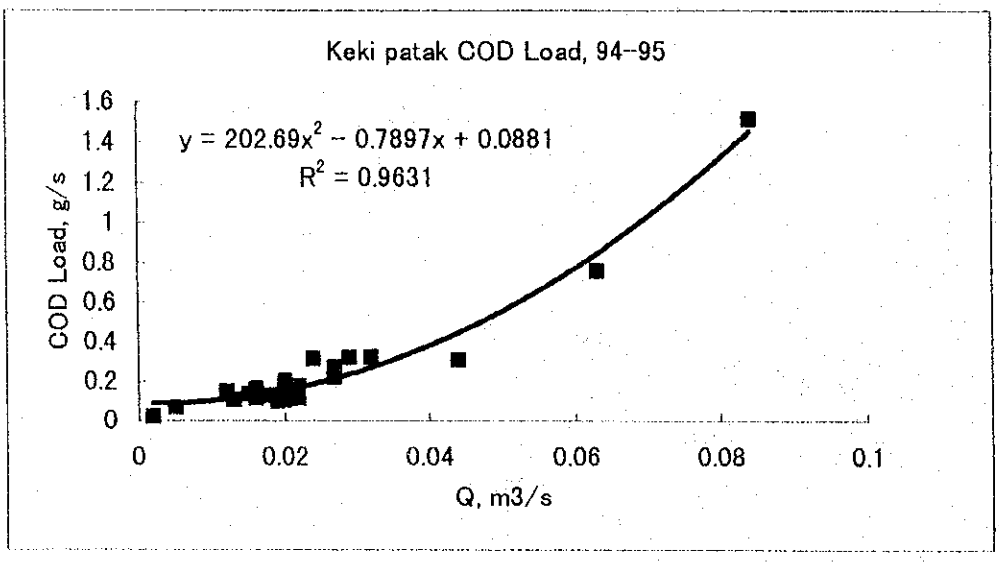

Figure B.5 Best Fit Curve for Load-discharge Correlations (Keki)

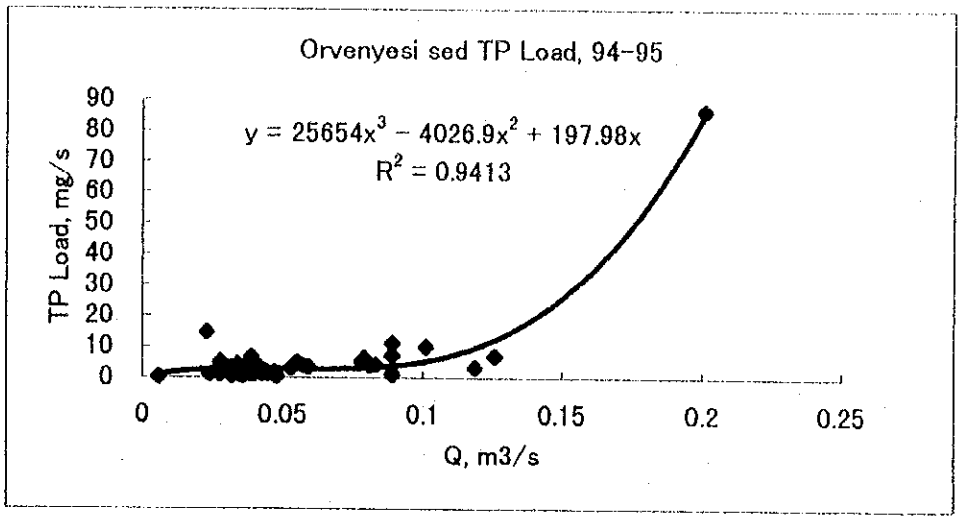

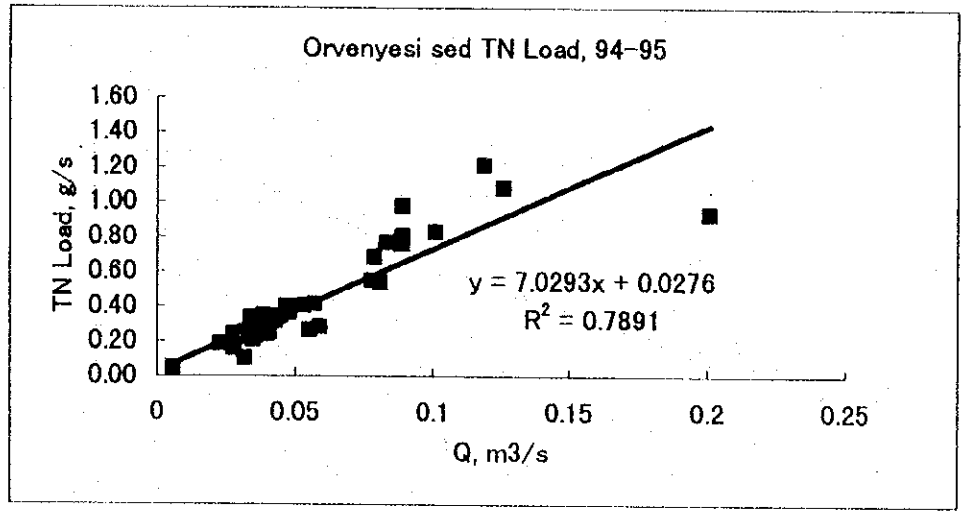

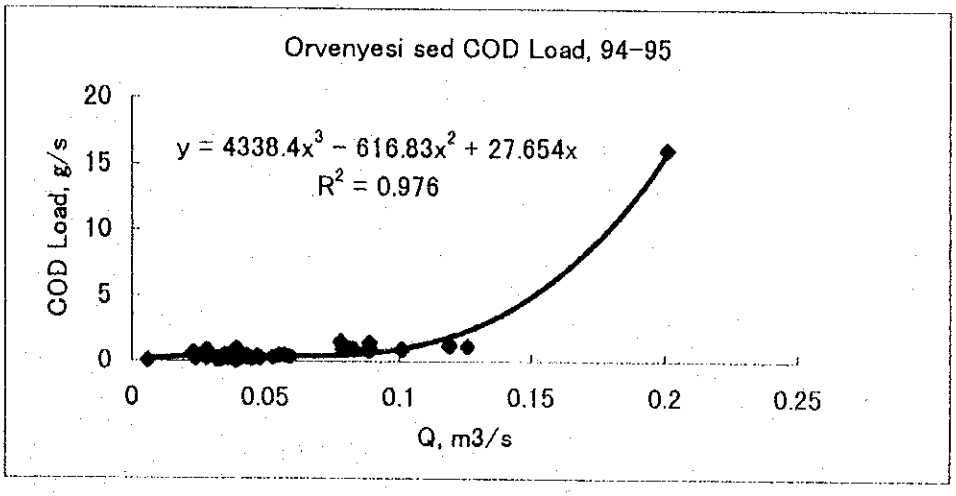

Figure B.6 Best Fit Curve for Load-discharge Correlations (Orvenyesi)

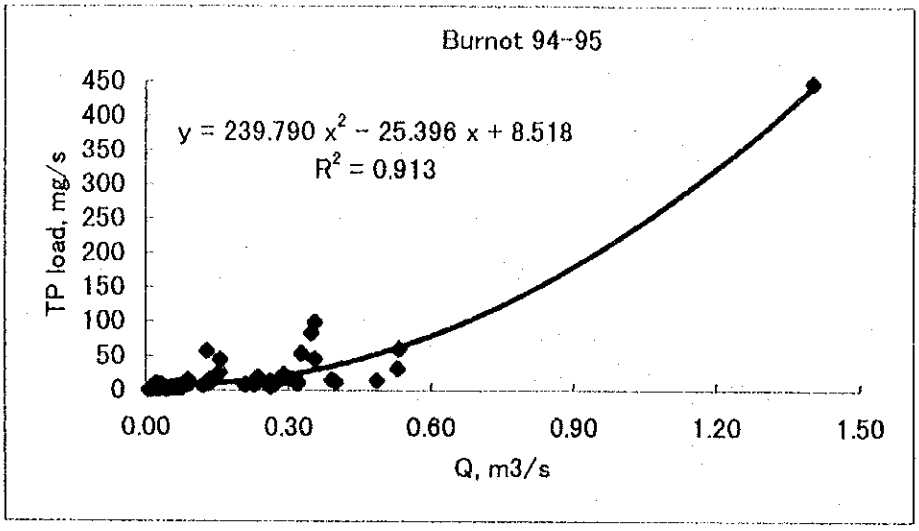

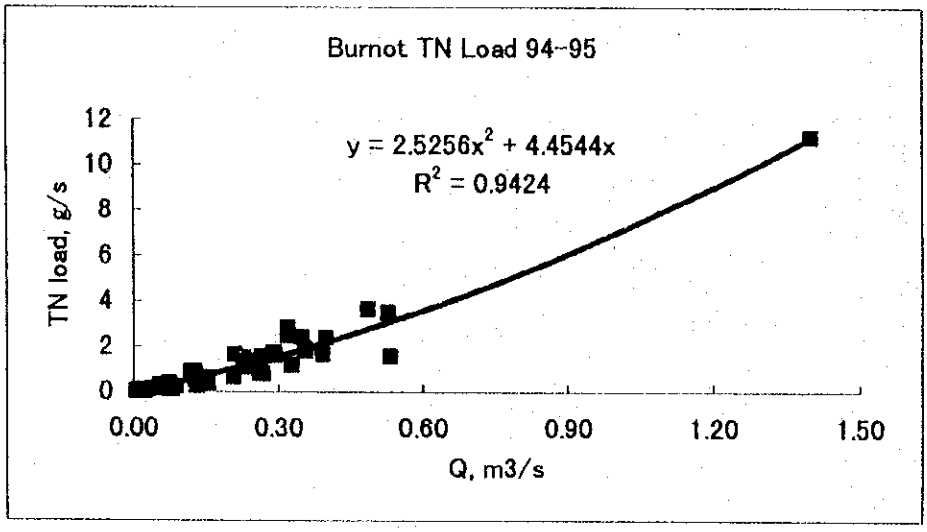

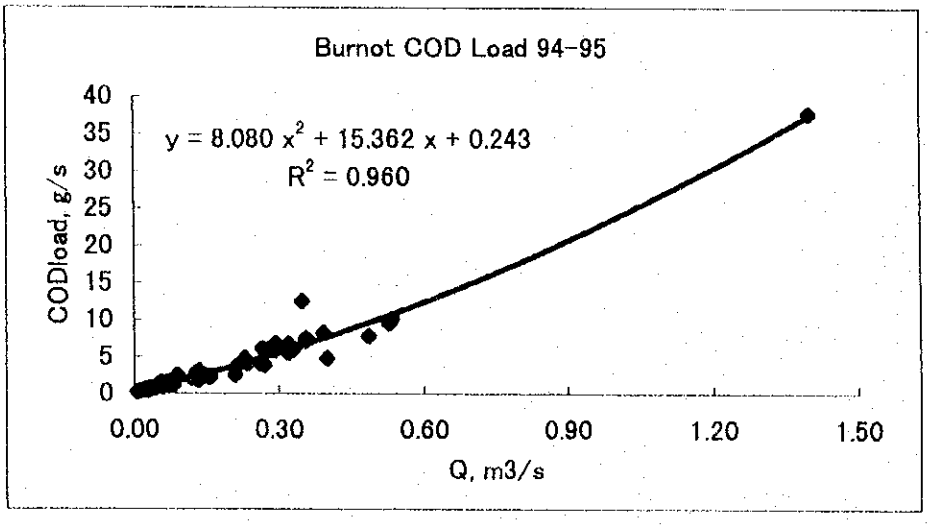

Figure B.7 Best Fit Curve for Load-discharge Correlations (Burnot)

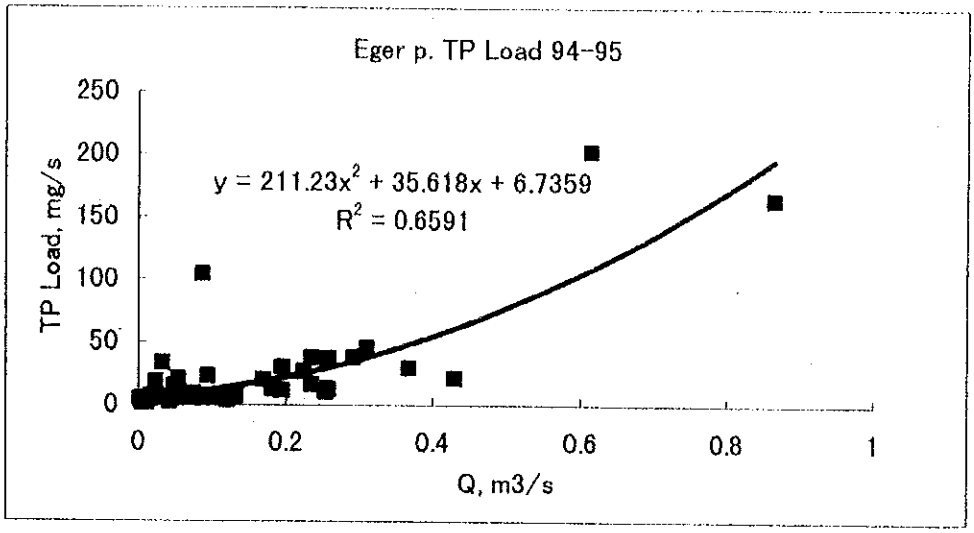

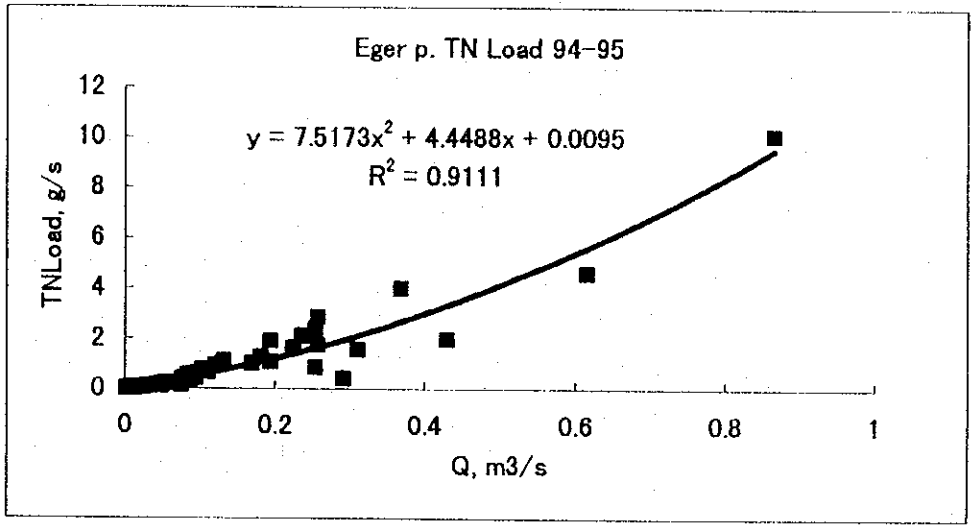

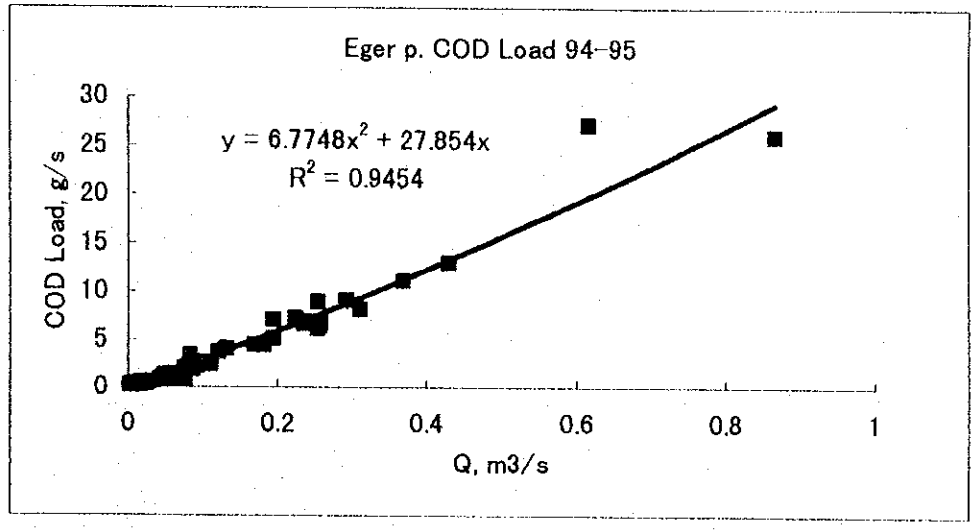

Figure B.8 Best Fit Curve for Load-discharge Correlations (Eger)

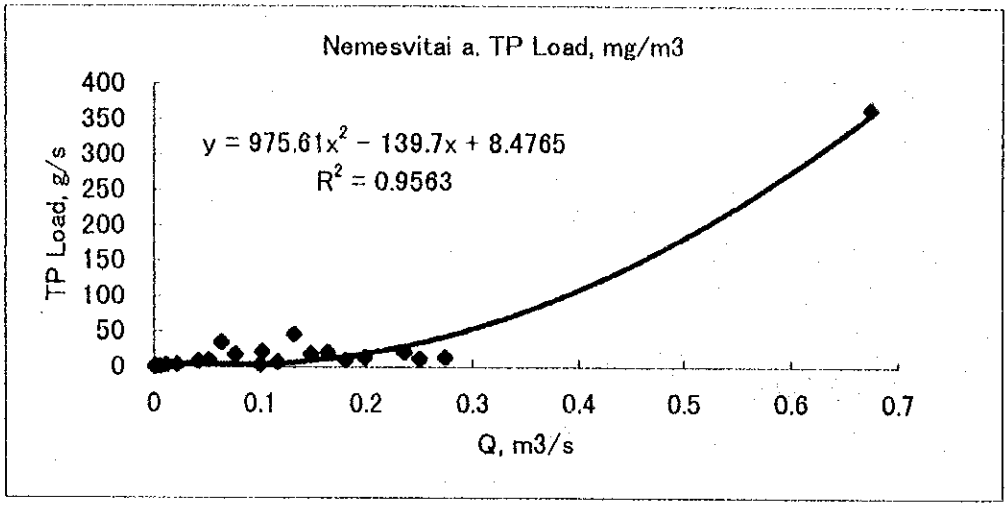

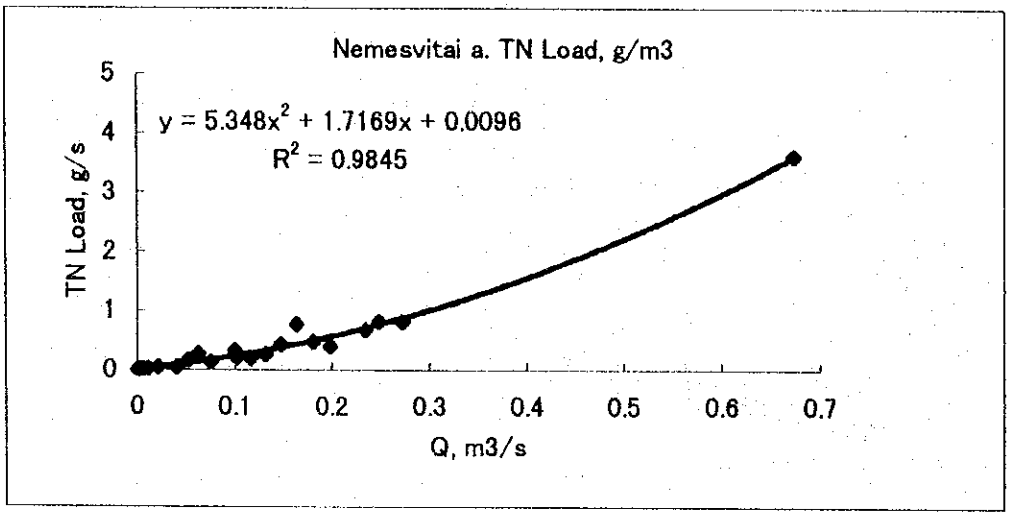

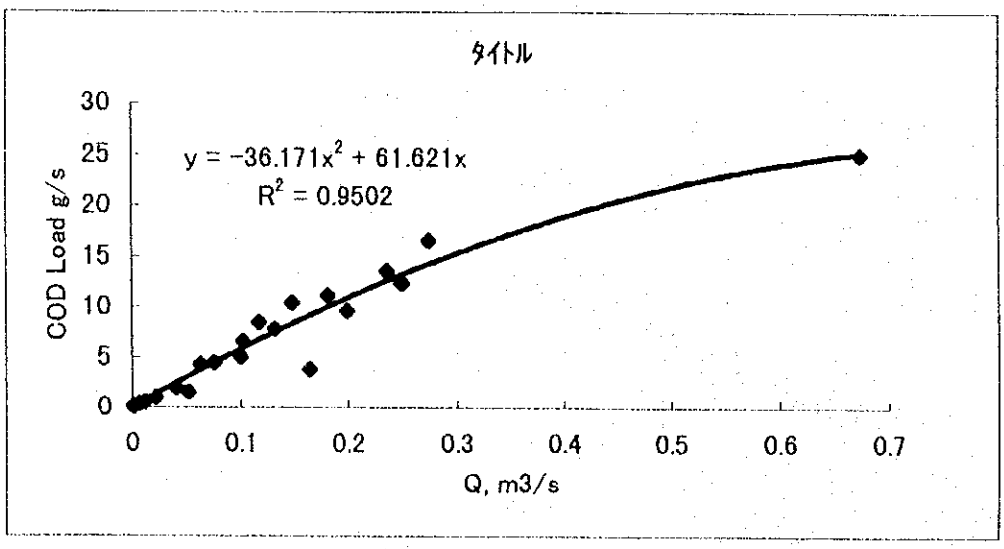

Figure B.9 Best Fit Curve for Load-discharge Correlations (Nemesvitai)

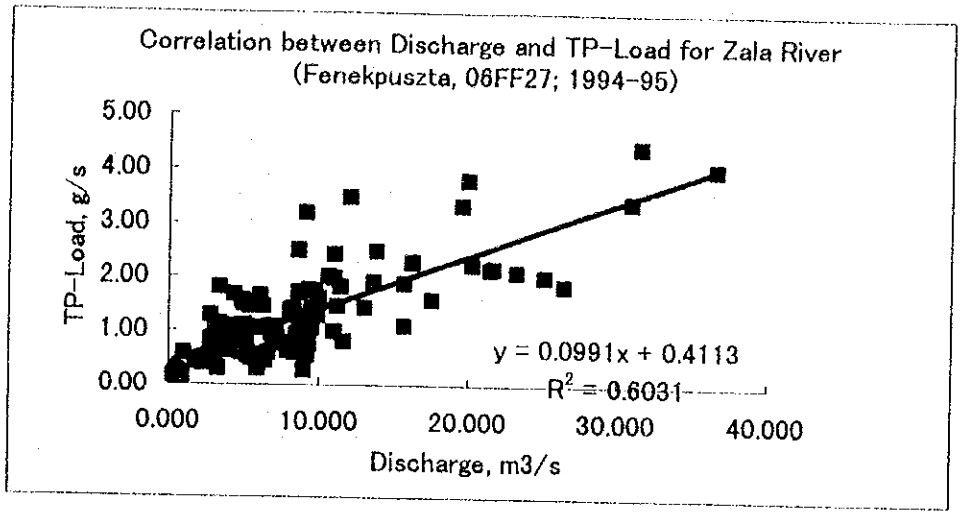

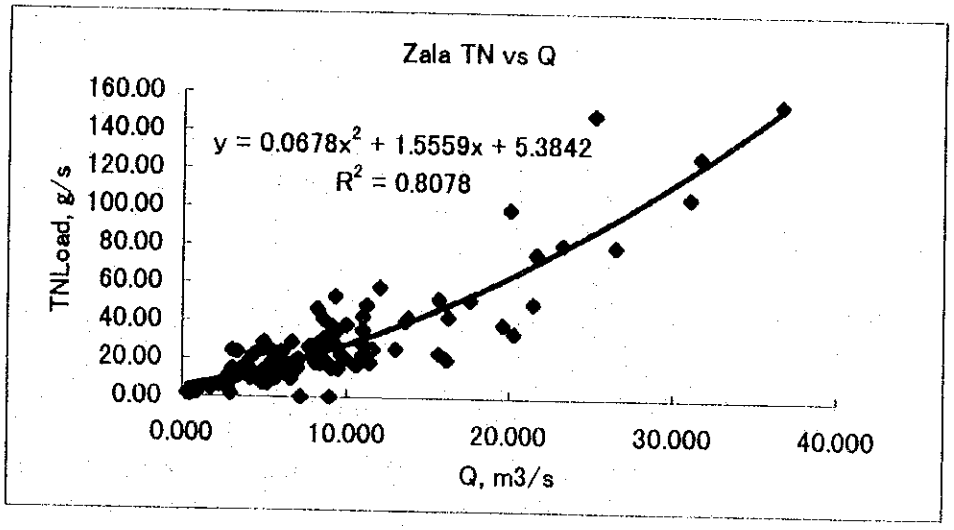

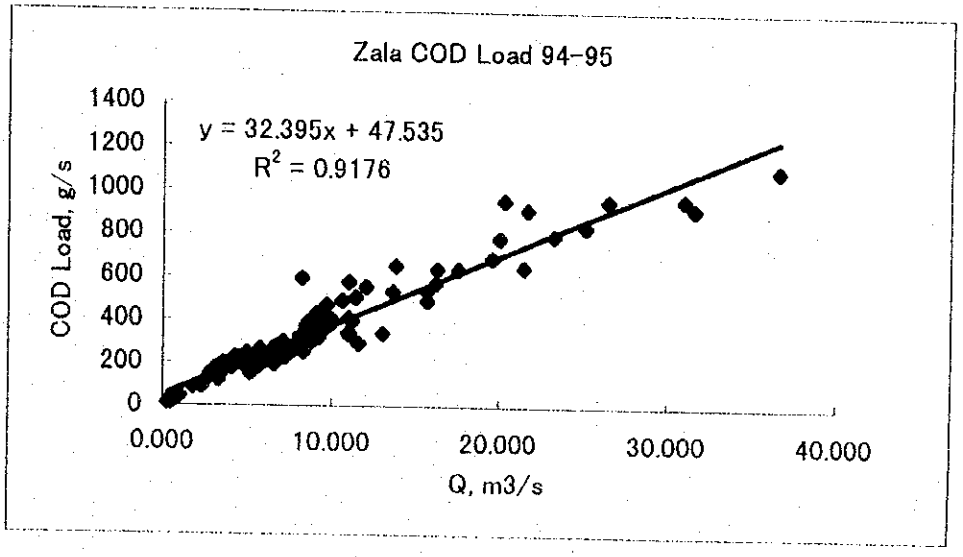

Figure B.10 Best Fit Curve for Load-discharge Correlations (Zala)

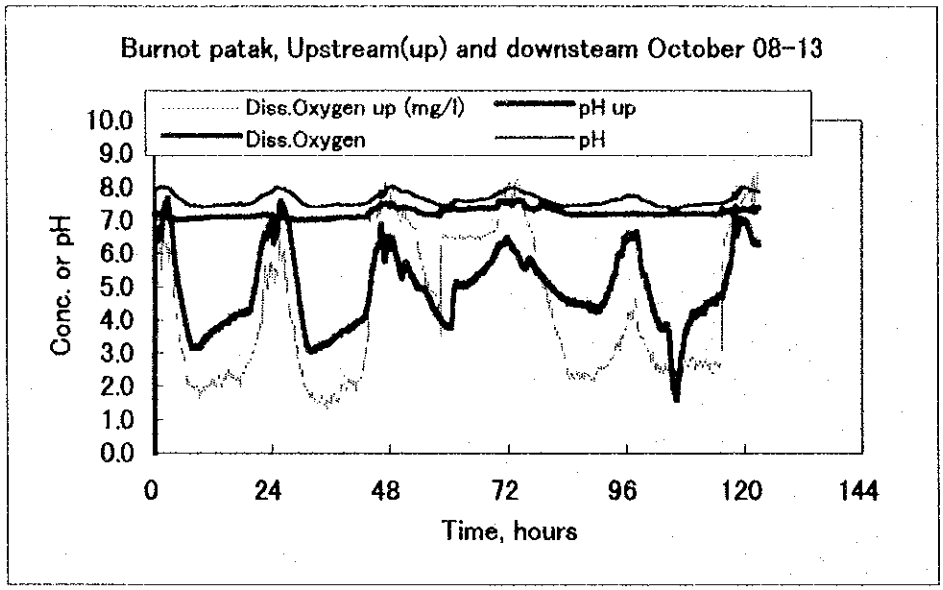

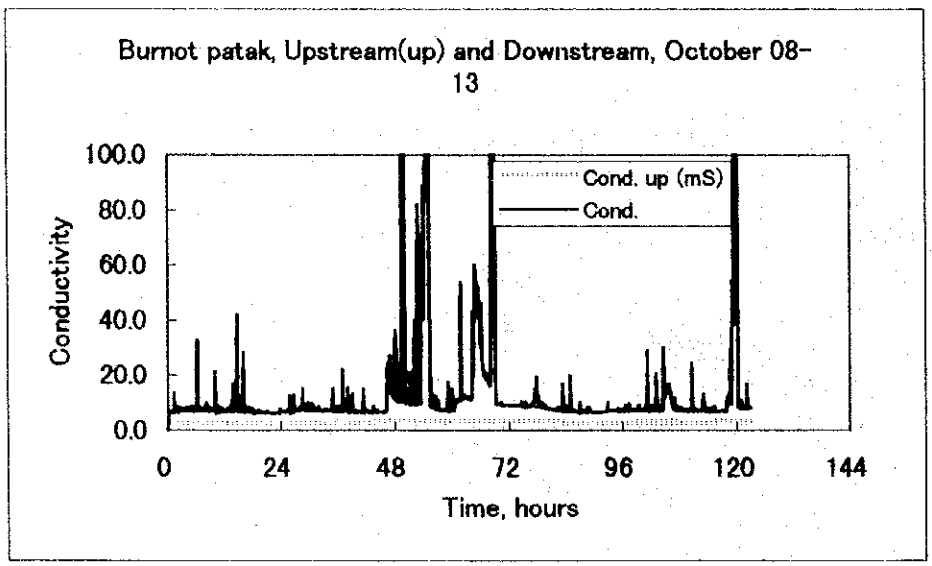

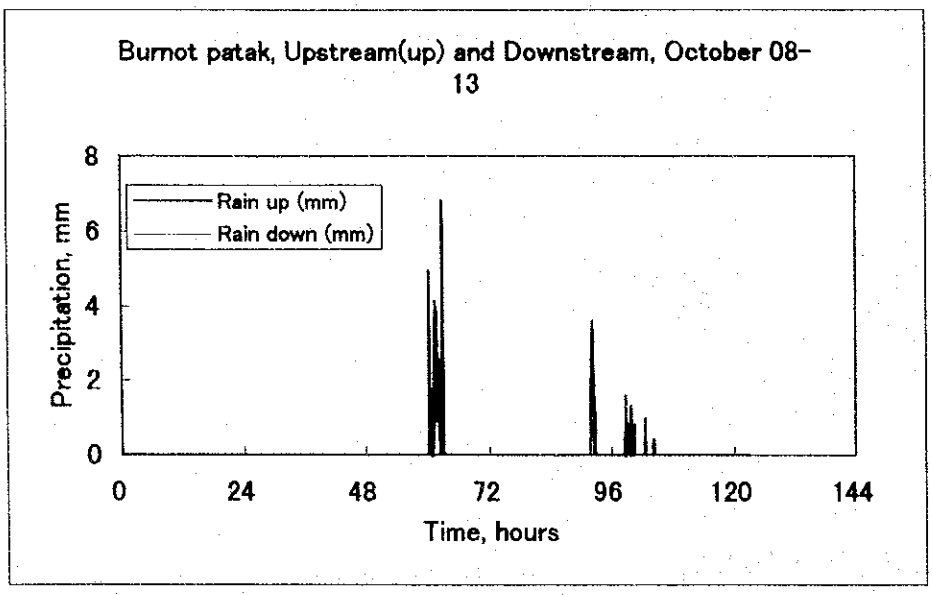

Figure B.11 Comparison of Upstream and Downstream Monitoring Data of Burnót Patak (1)

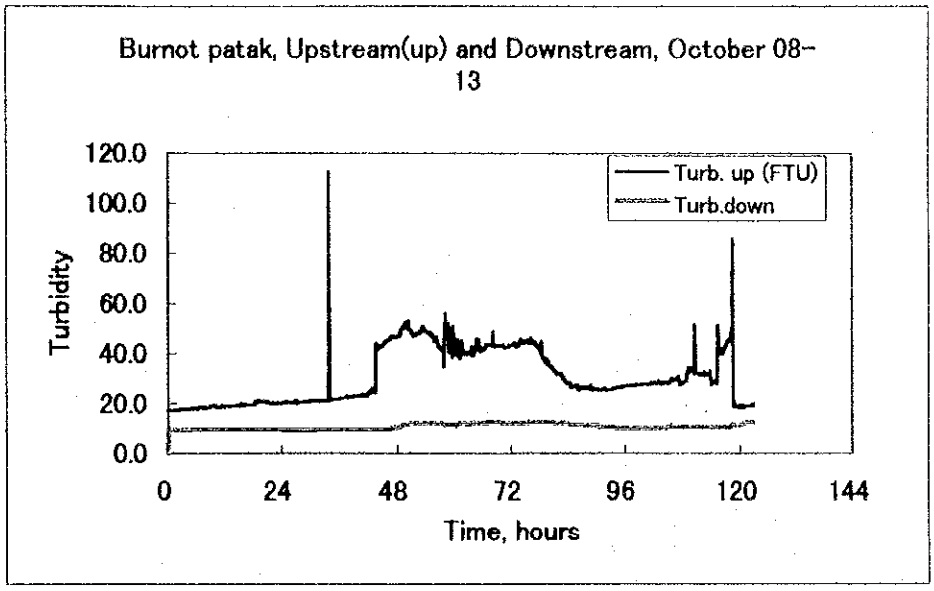

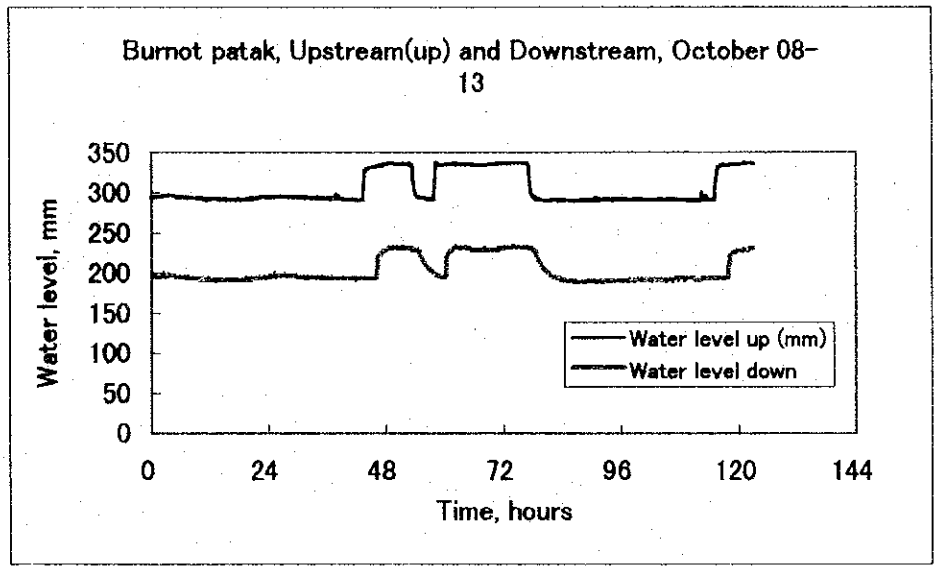

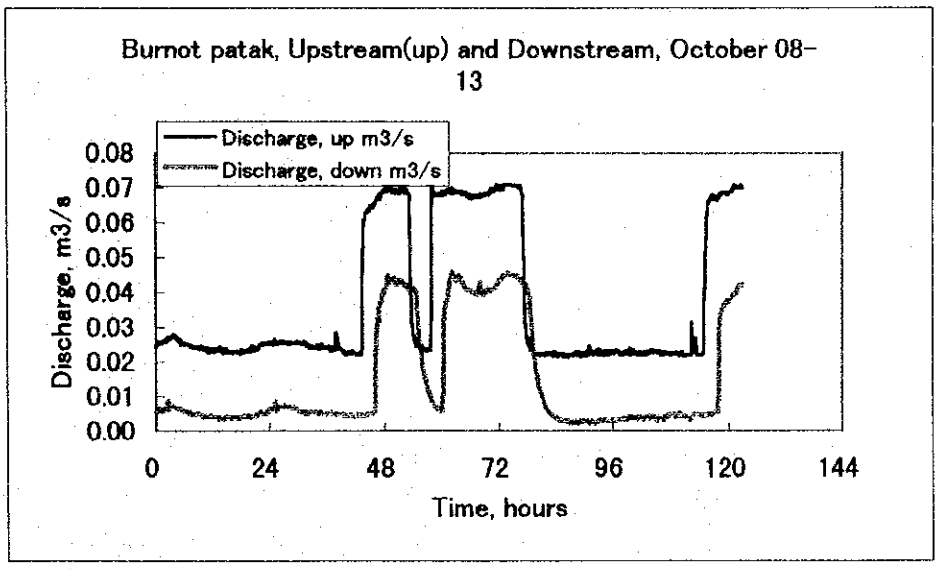

Figure B.12 Comparison of Upstream and Downstream Monitoring Data of Burnót Patak (2)

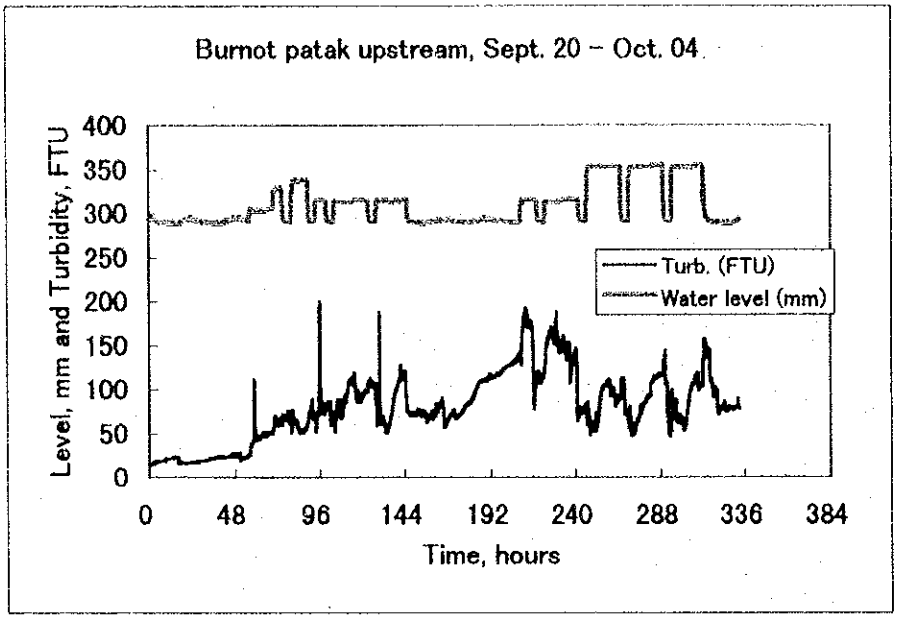

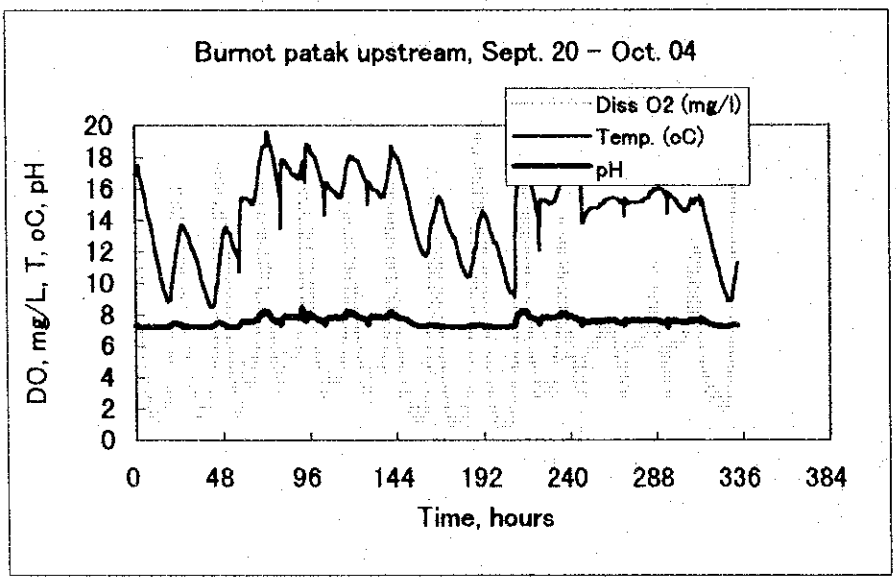

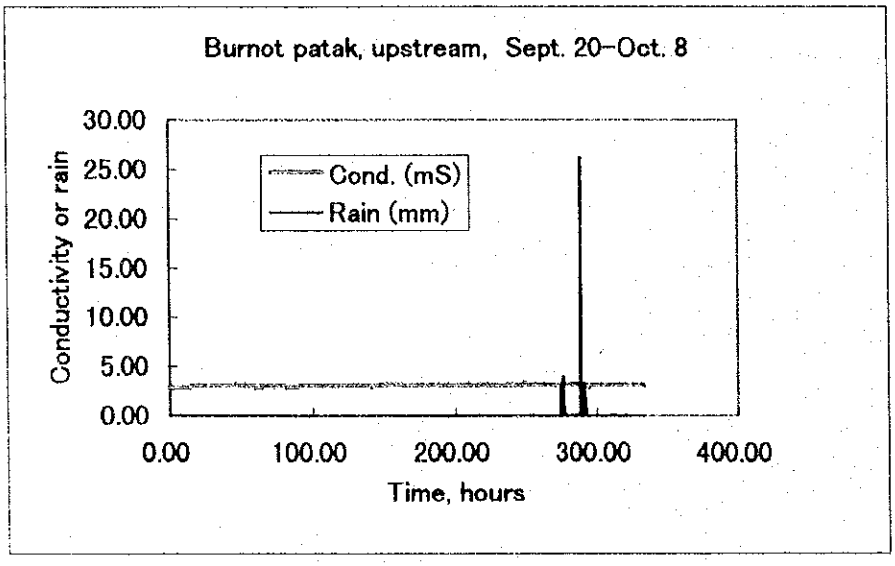

Figure B.13 Monitoring Data for Upstream Station of Butnót Patak

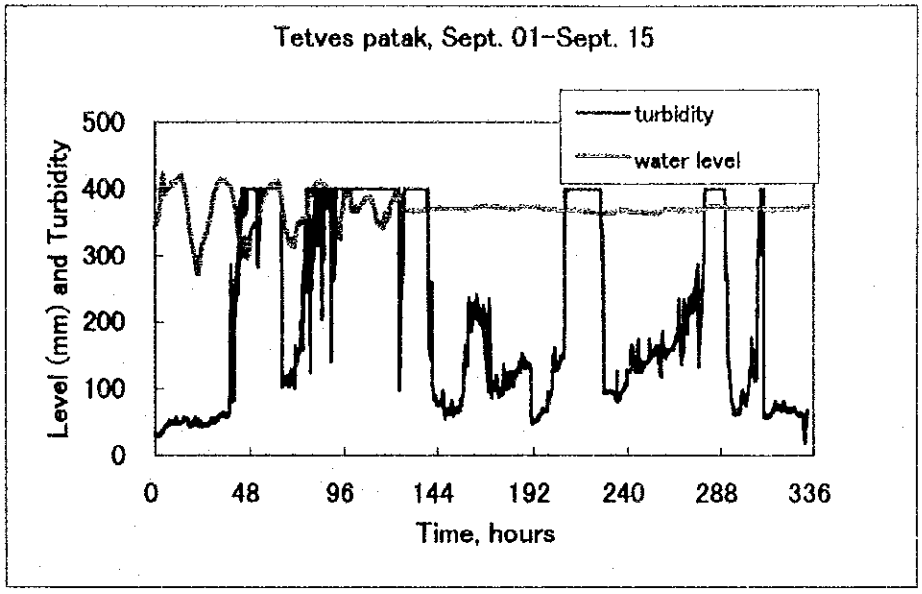

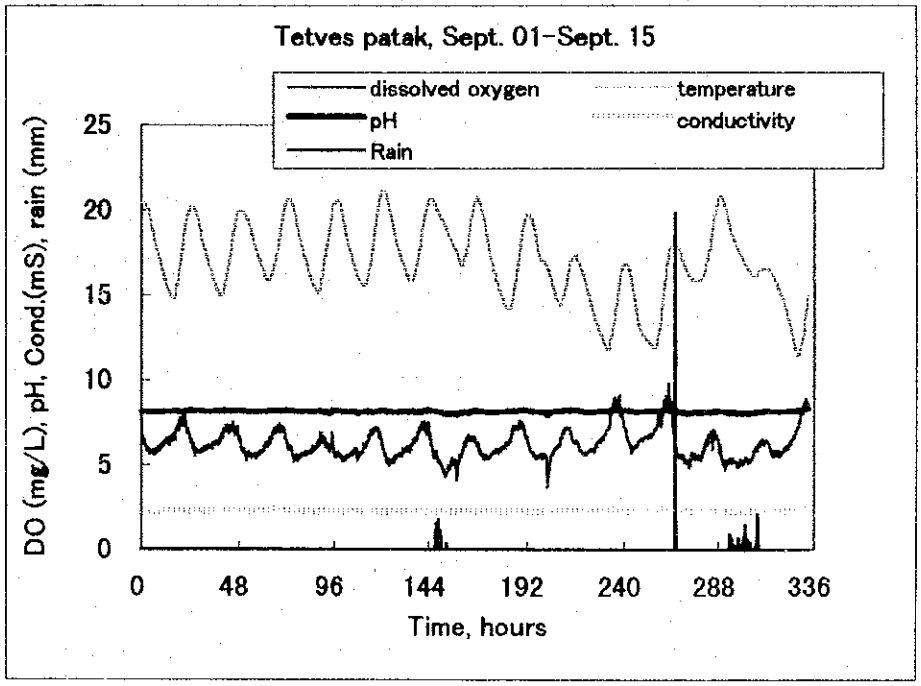

Figure B.14 Monitoring Data for Tetves Patak

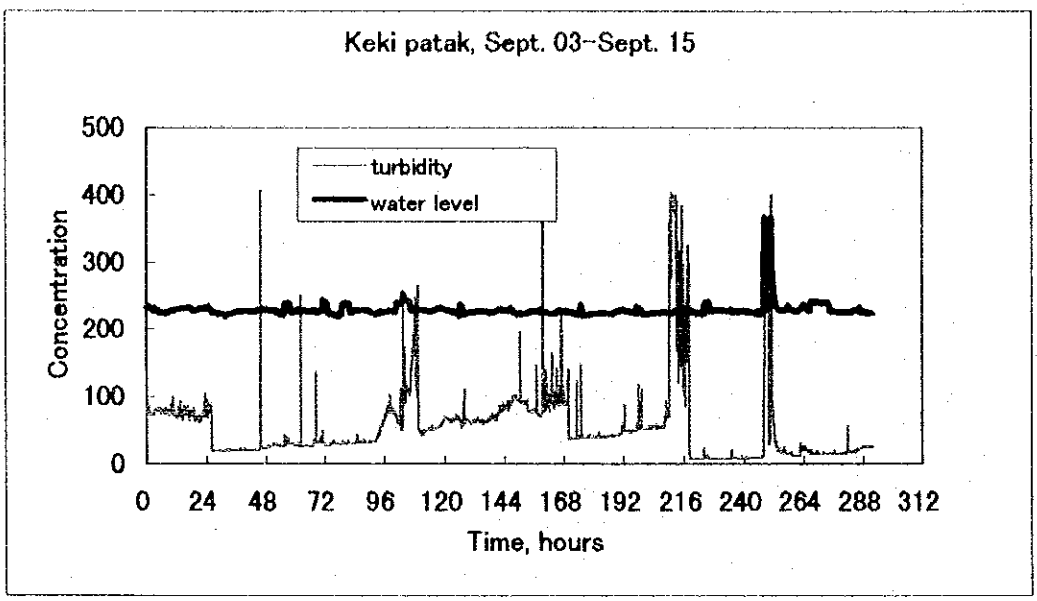

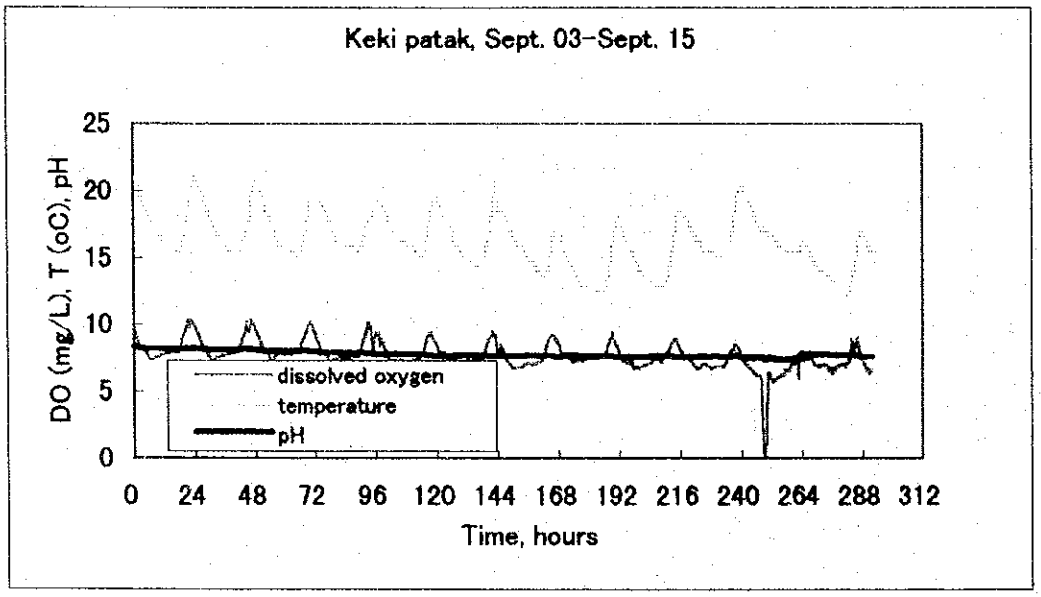

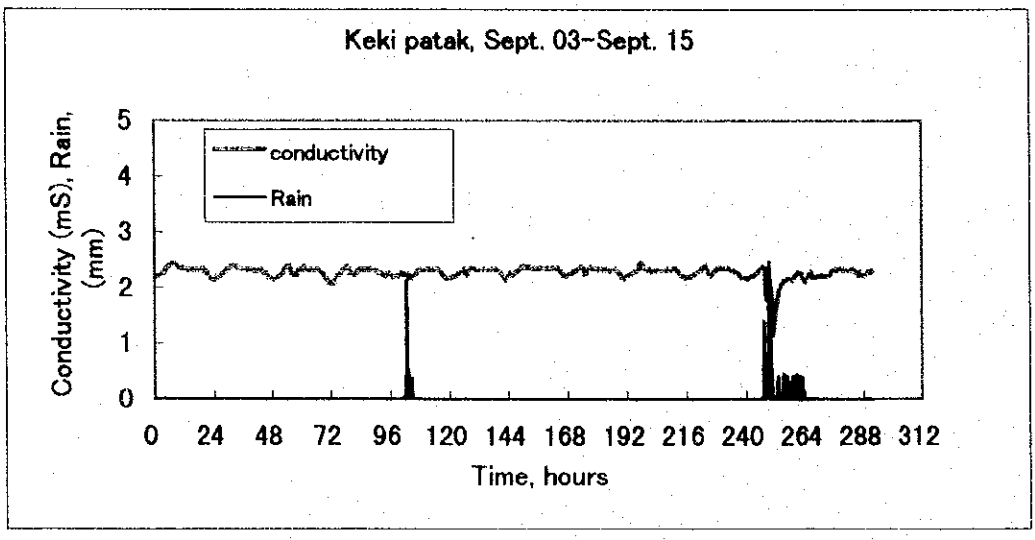

Figure B.15 Monitoring Data for Kéki Patak

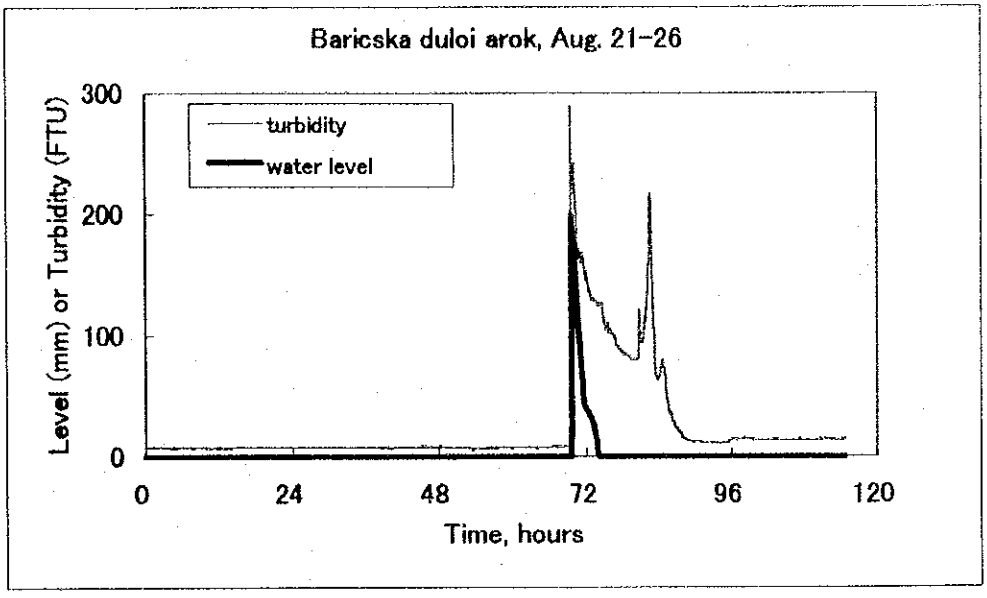

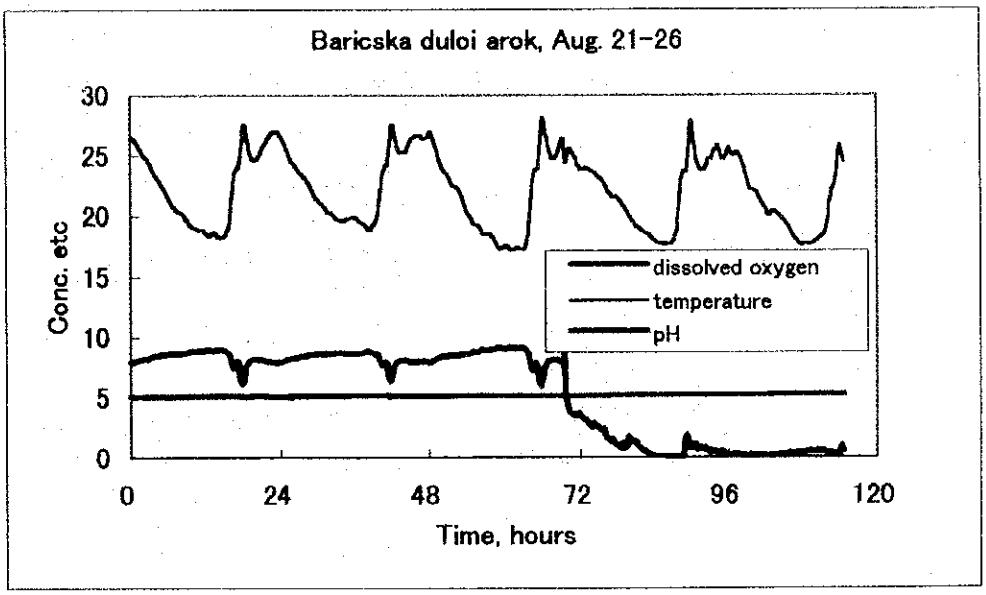

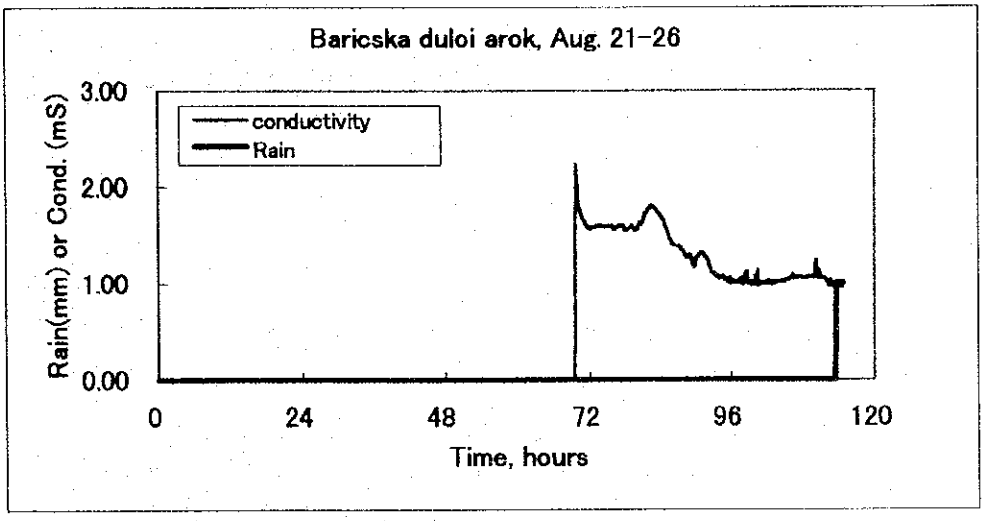

Figure B.16 Monitoring Data for Baricska Dûlôi Árok

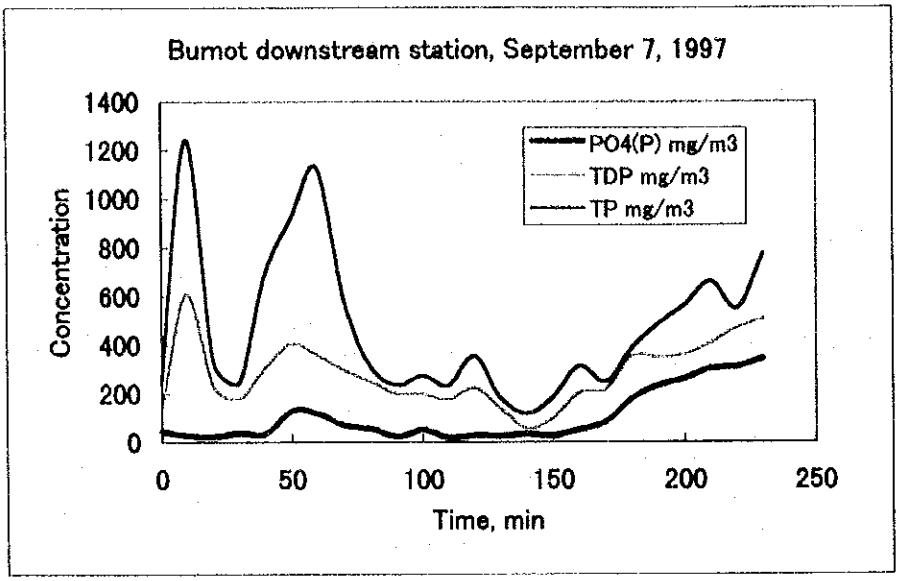

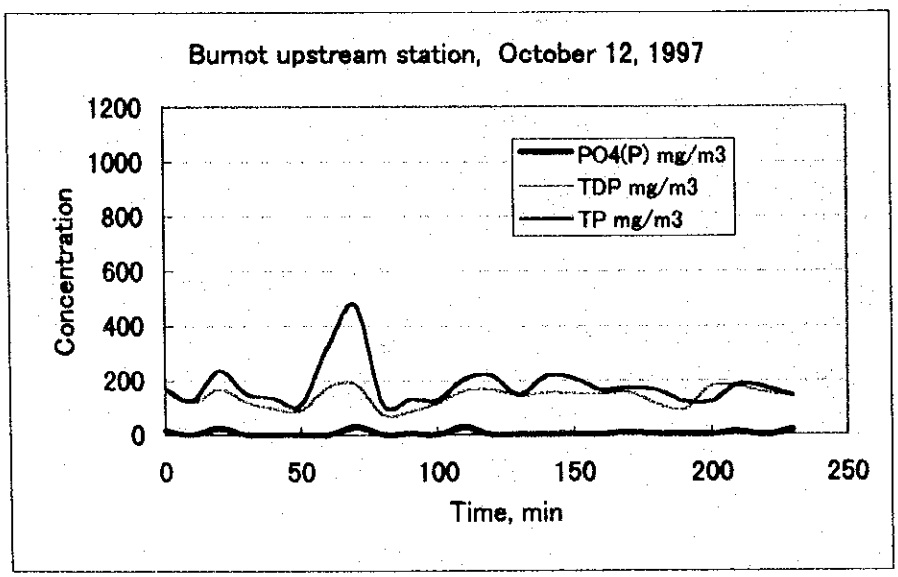

Figure B.17 Comparison of the Concentration of Various Phosophorous Forms at the Automatic Sampling Stations on Burnot Patak

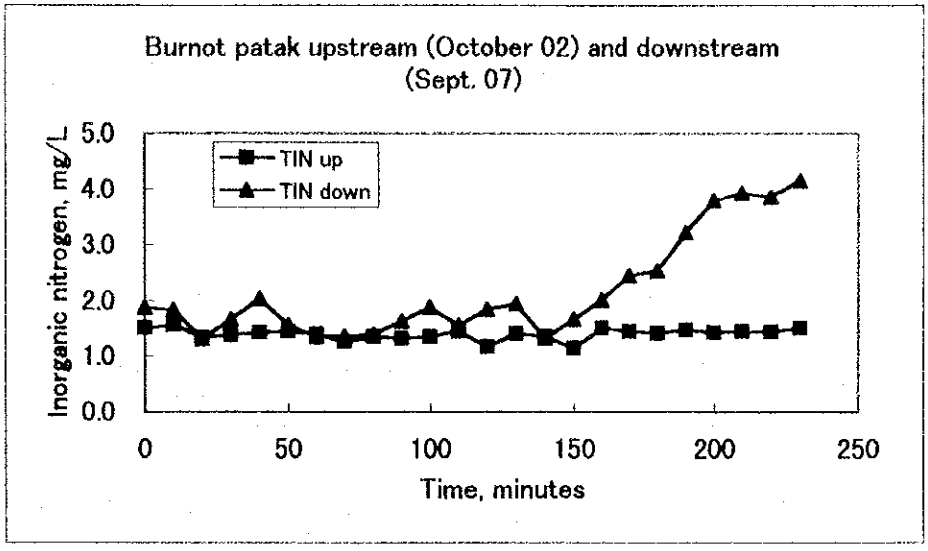

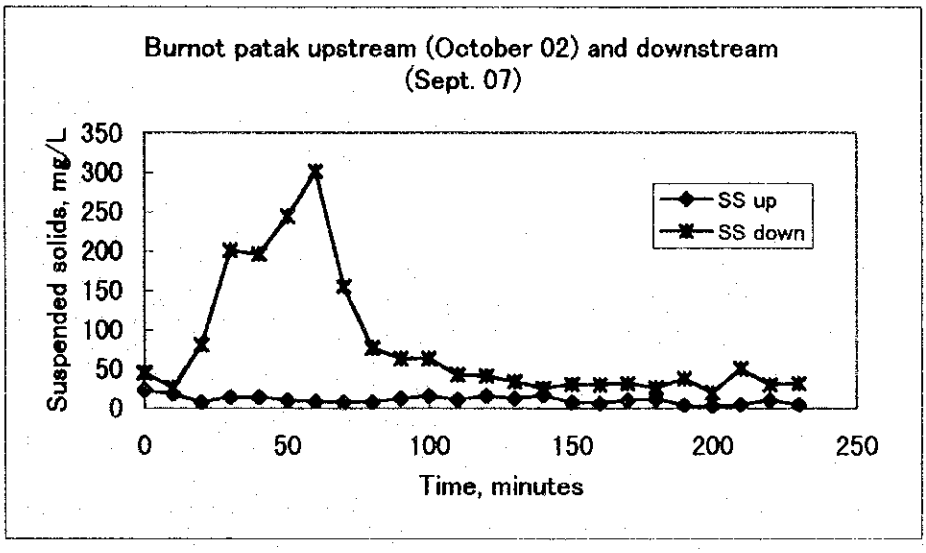

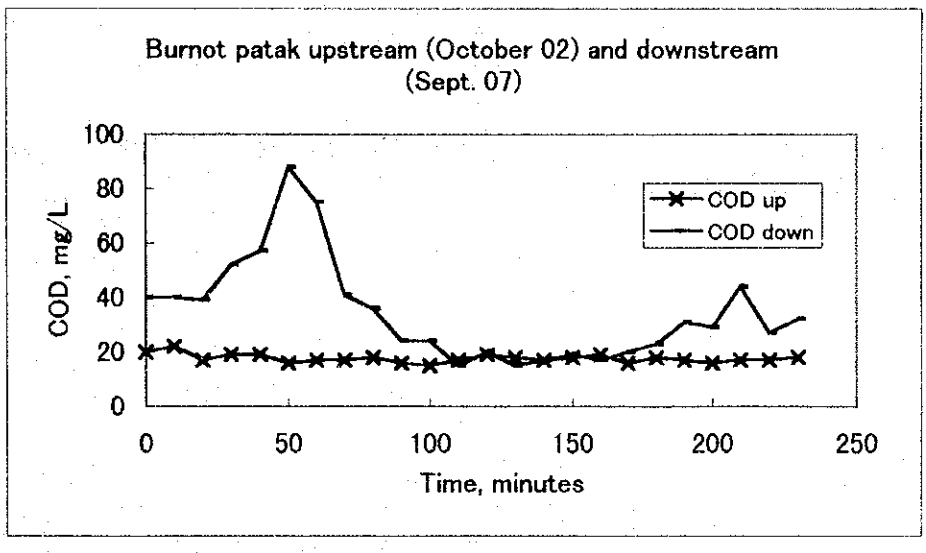

Figure B.18 Comparison of Water Quality of the Upstream and Downstream Automatic Sampling Stations on Burnot Patak

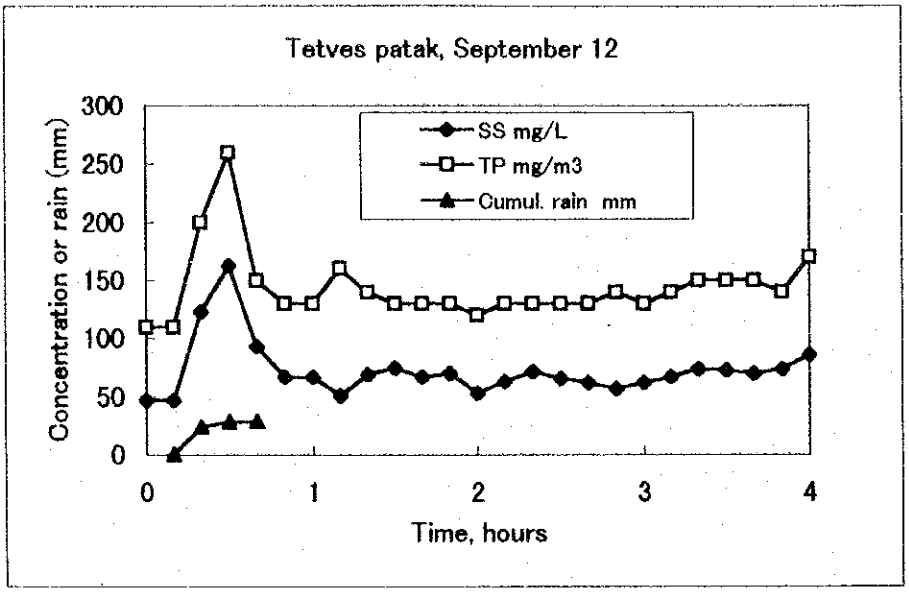

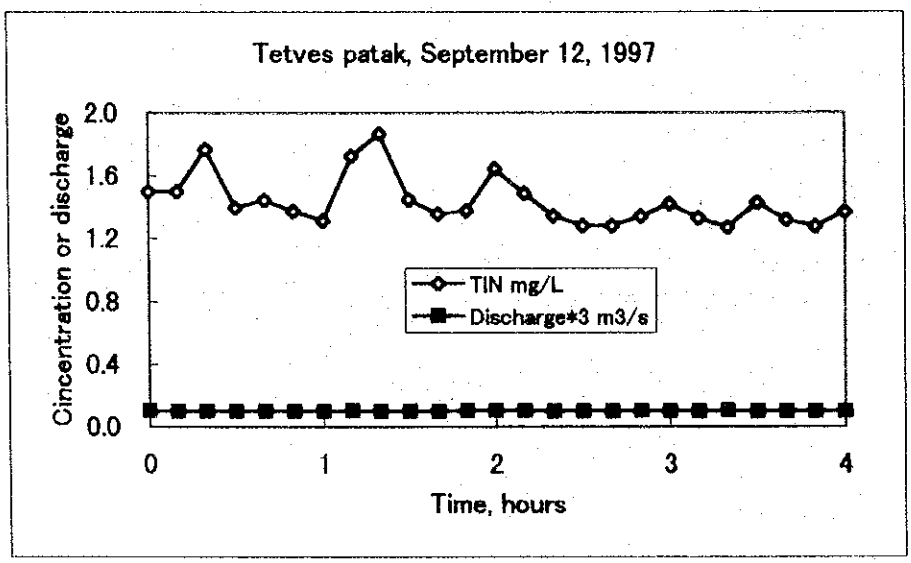

Figure B.19 Change of Water Quality and Discharge of Tetves Patak During a Minor Rain Event

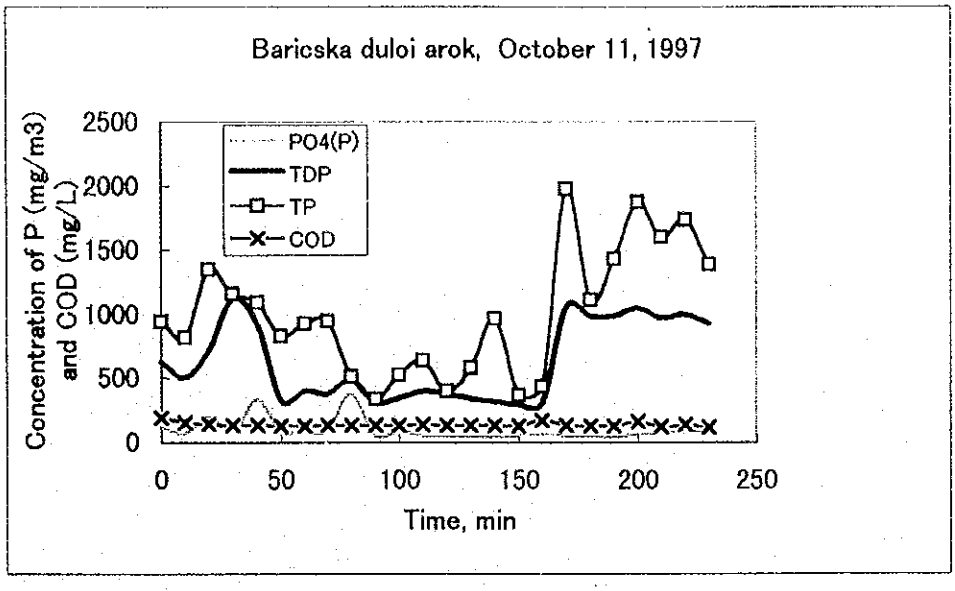

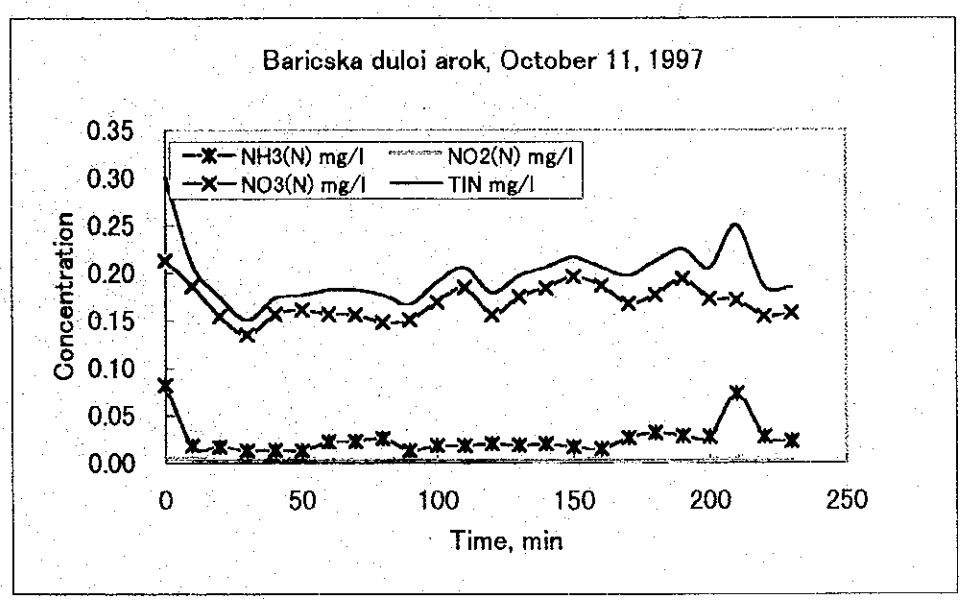

Figure B.20 Water Quality of Baricska Duloi Arok (No-flow Conditions)

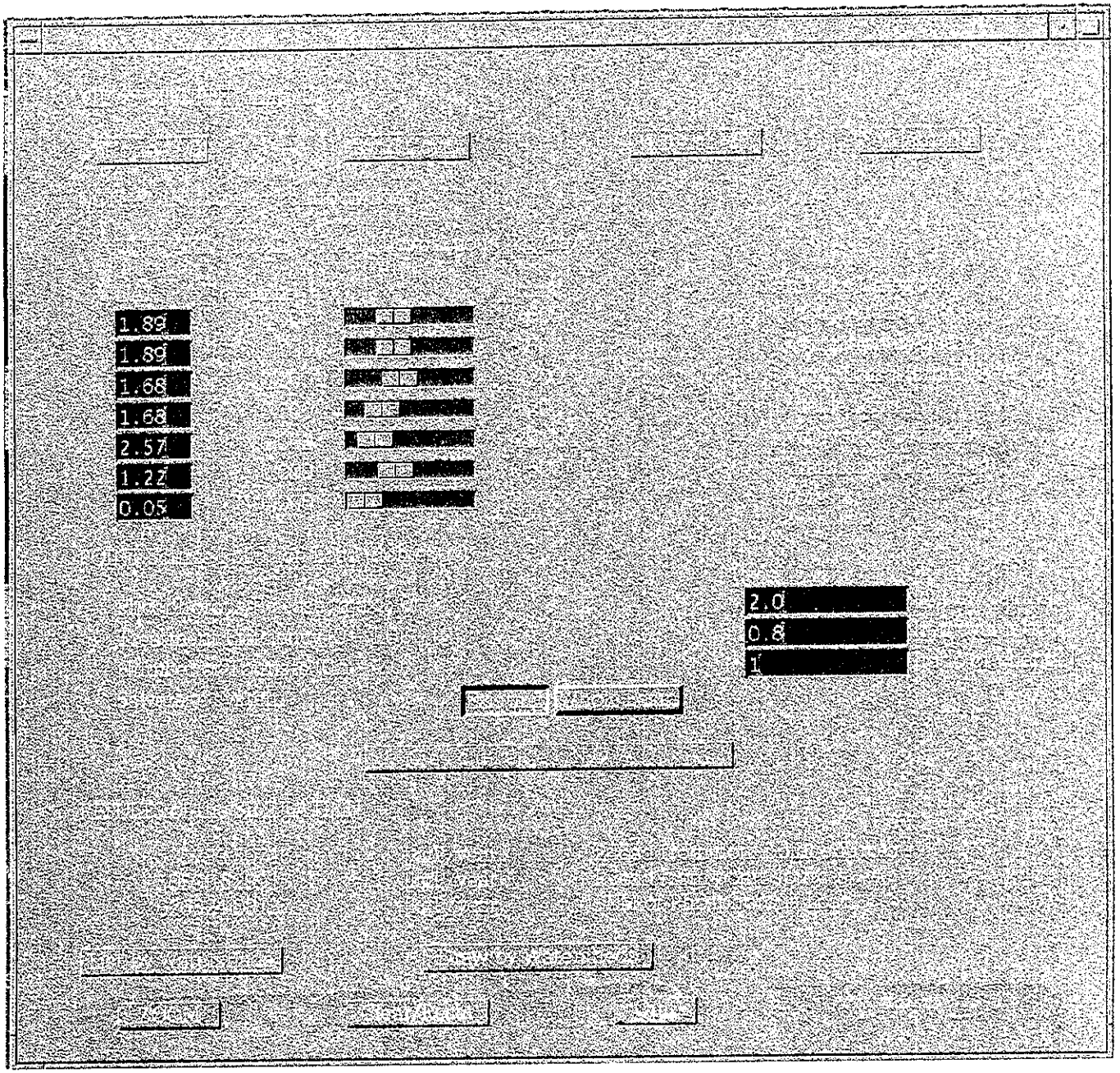

Figure B.21 "Control Panel" of a Simple Pollutant Load Estimation Module

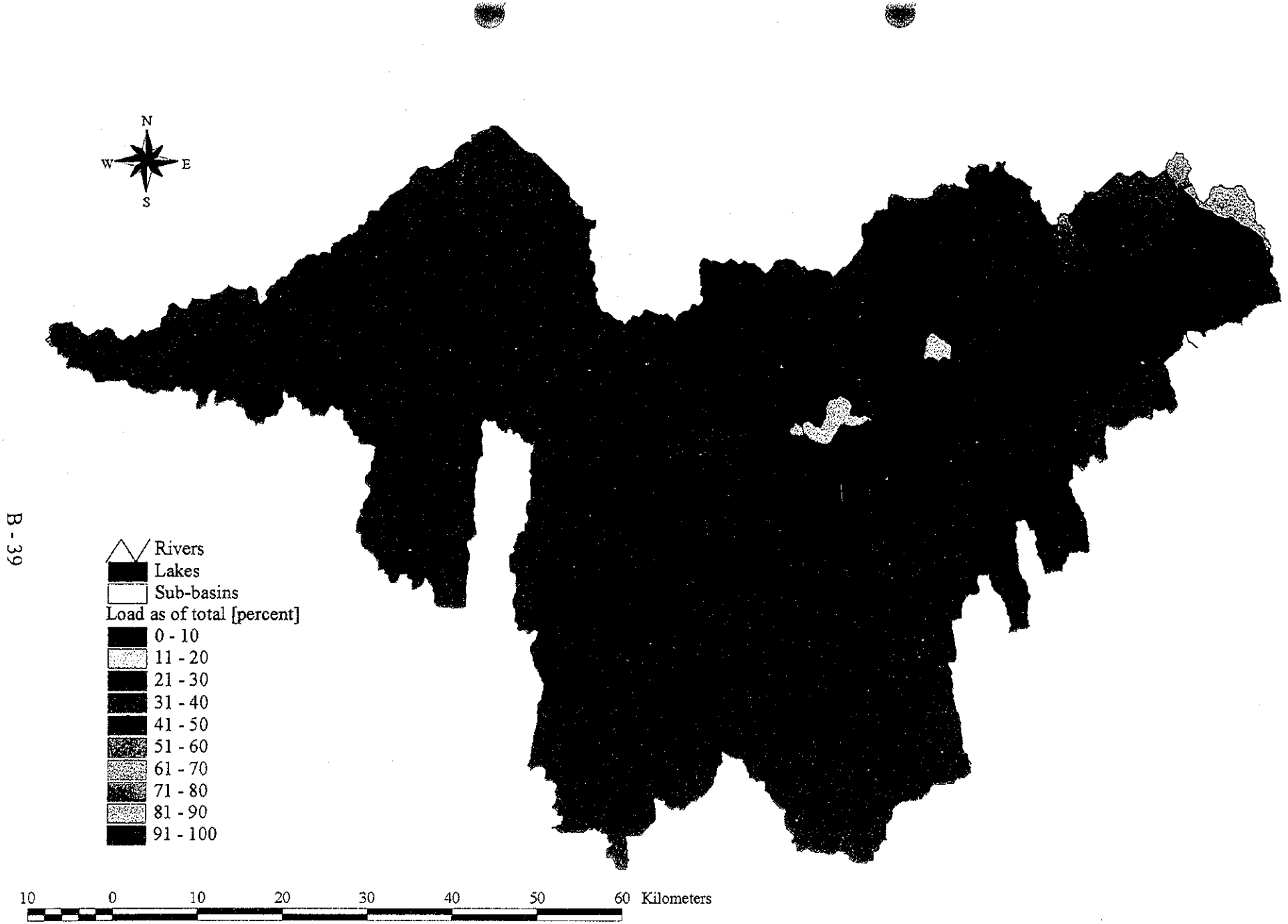

Figure B.22 Study of Non-point source Reduction Efficiency by Sub-watersheds

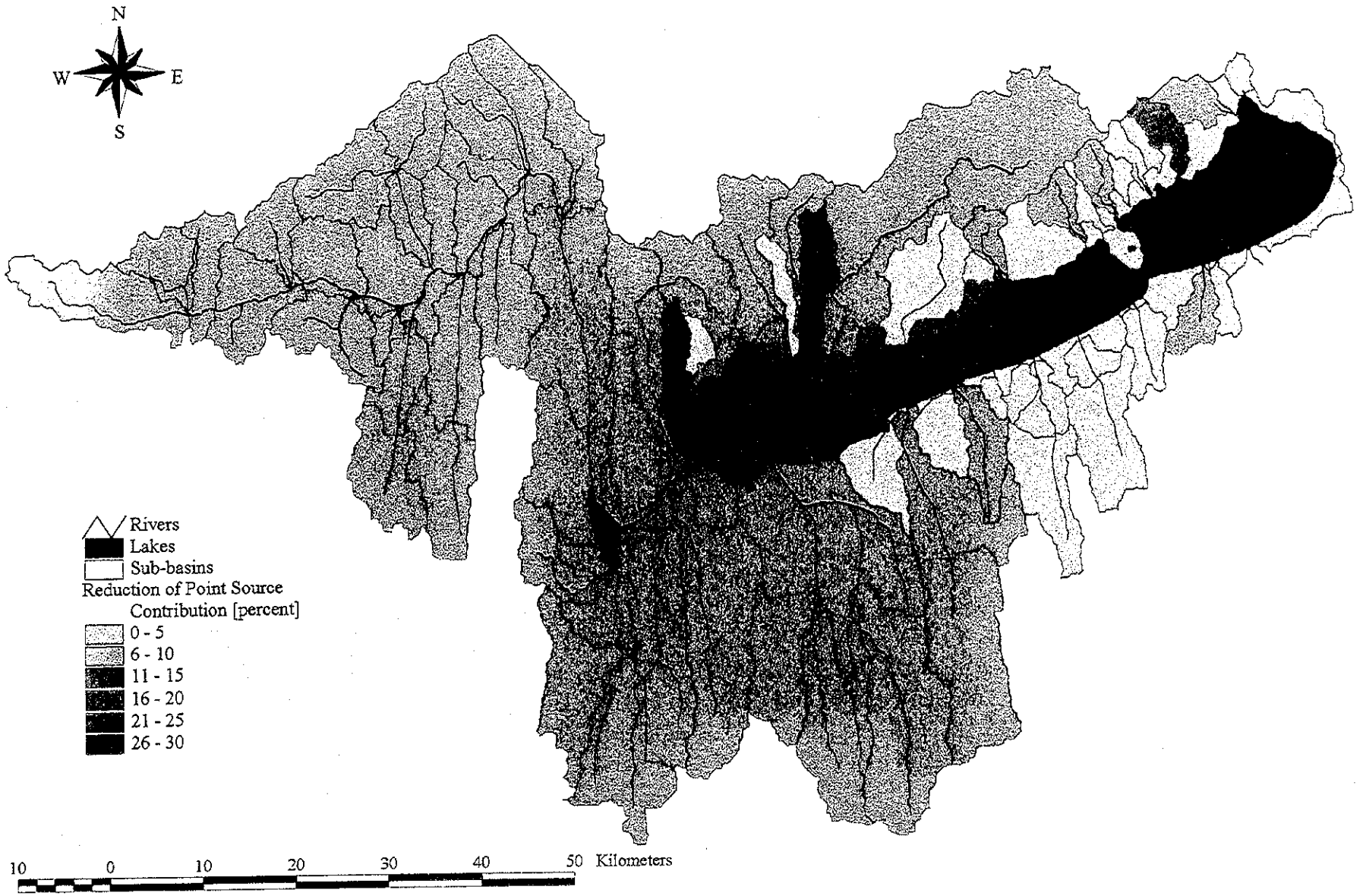

Figure B.23 Study of Sewage Treatment Upgrading Efficiency by Sub-watersheds

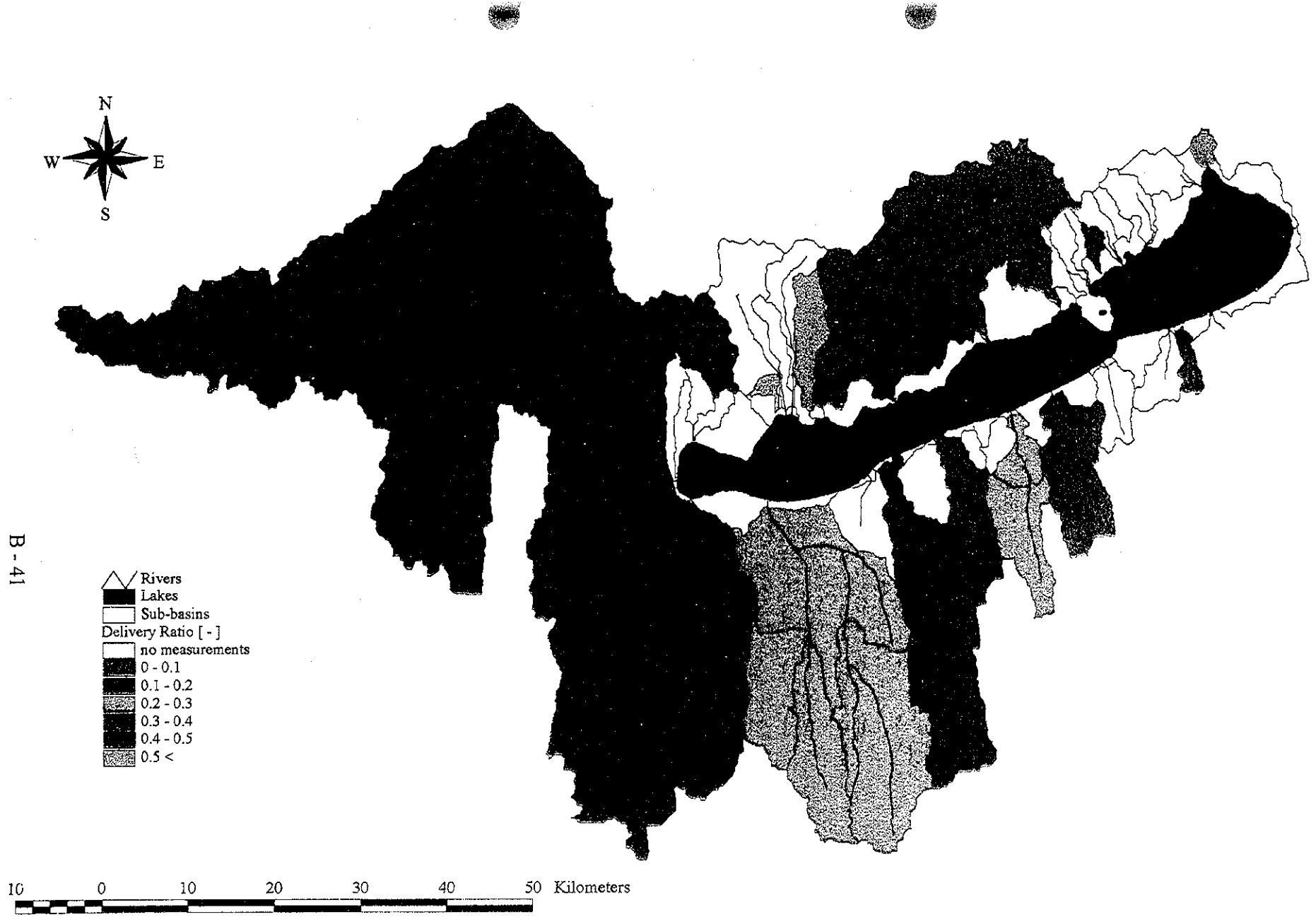

Figure B.24 Determination of Pollutant Delivery Ratios of the Individual Sub-watersheds

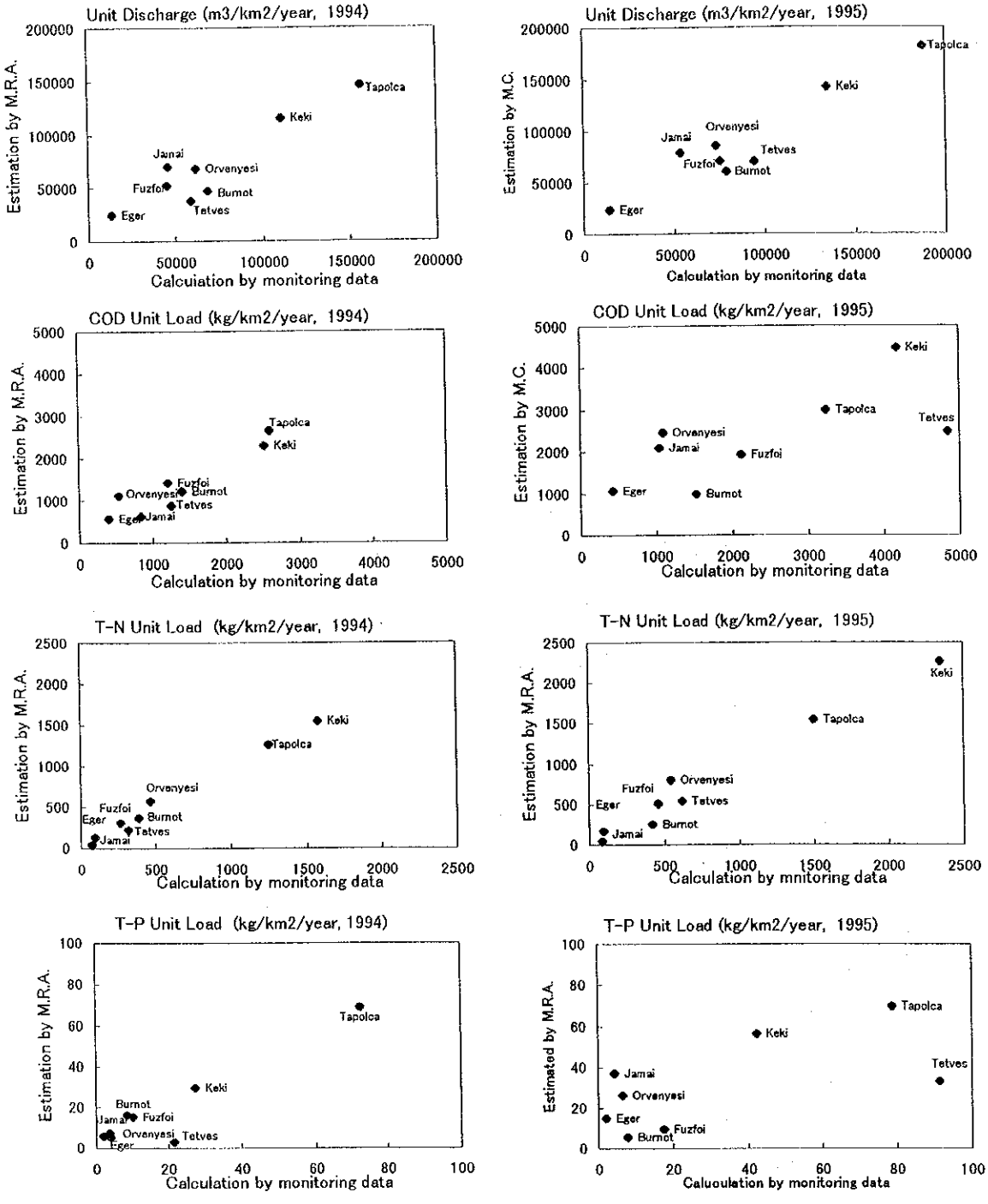

Discharge94 :Y=31700(P)-2620(L)+42700(S)-2460(T)+51600
COD94 :Y=891(P)-38.2(L)+3130(S)-29.9(E)-20.9(T)+1550
T-N94 :Y=660(P)+5.91(L)+3630(S)+12.4(E)-29.1(T)-1940
T-P94 :Y=22.8(P)-0.615(L)-16.8(S)-0.775(E)-0.707(T)+29.2

Discharge95 :Y=37800(P)-4230(L)+16500(S)-3040(T)+91400
COD95 :Y=741(P)-21.2(L)+3270(S)-39.8(E)-62.3(T)+1750
T-N95 :Y=797(P)+3.62(L)+4690(S)+1.34(E)-36.0(T)-2080
T-P95 :Y=15.4(P)-0.168(L)-28.7(S)-0.845(E)-1.93(T)+65.9

P :Population density (person/ha)
L :Avarage length of the basin (km)
S :Ratio of area more than 3deg. Slope (%)
E :Avarage of soil erosion possibility (%)
T :Ratio of residential use and recreational use area (%)

Figure B.25 Multiple Regression Analysis (1994 & 1995)

APPENDIX - C

LAKE BALATON WATER QUALITY SIMULATION MODEL

APPENDIX - C

LAKE BALATON WATER QUALITY SIMULATION MODEL

Page

CONTENTS

LIST OF TABLES

LIST OF FIGURES

APPENDIX - C

LAKE BALATON WATER QUALITY SIMULATION MODEL

1. ANTECEDENTS

The phenomenon of eutrophication is more irregular in character and less satisfactorily understood for shallow bodies of water, such as *Lake Balaton*, than that for deeper lakes. In the late 1970s, the *International Institute for Applied System Analysis* (*IIASA*) initiated a program on studying the eutrophication processes in shallow lakes with particular interest focused on *Lake Balaton* as the subject of a case study. There were three main considerations which prompted the earlier *Lake Balaton* case studies: 1) fairly large amount of data was available from the precedent Hungarian research activities; 2) the lake possesses the "typical" properties of shallow lakes in many respects; and 3) since serious economic interests are involved in the abatement of the eutrophication processes, "practical" questions had to be dealt with rather than, or in addition to, the scientific issues. These aspects of *Lake Balaton* research still remain pertinent today after more than a decade.

The cooperative study involving *IIASA*, the *Hungarian Academy of Sciences*, the *National Water Authority*, the *Balaton Limnological Research Institute*, and the associated establishments, continued into the mid-1980s with a considerable vigor, when the transition of the political and economic scheme seem to have disrupted further collaborative effort. Although the research and monitoring efforts by the individual institutes and organizations have persisted, their inter-institutional consequences have not frequently surfaced in the public scene.

The conditions related to the water quality of *Lake Balaton* have undergone significant transformations during the past two decades. The changes in the conditions of the lake drainage basin resulting from the economic, industrial, and agricultural transformations, as well as the land-use practice, are among the most significant factors of pertinence. In 1994, alarmed by an explosive blue-green algal bloom of an unprecedented scale, the *Central Transdanubian Environmental Inspectorate* (*KDT-KÖFE*) compiled a water quality time-series for the period 1975 to1994 (*KDT-KÖFE*, 1994).

Apart from the consistently increasing trend in *chlorophyll-a* (*Chla*) and the spread of hypertrophy eastward, no conclusive accounts pointing to the occurrence of the explosive bloom could be found. The report imputed antecedent effects of dry and warm climate to the probable cause of the bloom, without substantiation. The bloom occurred, according to the same report, despite the generally decreasing trend of phosphorous and nitrogen loads in recent years, although this statement cannot be verified by the record. The transitions of water quality and nutrients load conditions during the period 1984

to 1996 were also compiled by *KDT-KÖFE*, and some of the representative charts are shown in *Figures C.1* to *C.3*. The levels of PO_4-*P* concentration in the figures are conspicuously high, likely resulting from unsuitable analytical laboratory procedures as will be addressed in a later section.

The most noteworthy transformation, other than chemical indices, is exemplified by the conspicuous succession of dominant N_2-fixing phytoplankton species from *Aphanizomenon-* to *Anabena*-type, and to *Cylindrospermopis raciborskii*. *C. raciborskii*, a toxin producing blue-green, has been the predominant specie in the lake since 1982. In the years of significant algal blooms, 82, 84, 86, 88~90, 92 and 94, more than 85% of biomass had been attributed to *C. raciborskii* in all the sub-basins. Padisák and Istvánovics (1996) reported that the net rate of population increase was 0.24/*d* in 1992, and 0.27/*d* in 1994.

In 1992 and 94, *C. raciborskii,* of subtropical origin, was monodominant in the late summer peak at 90 to 95% of the total biomass. According to Padisák and Istvánovics (1996), *C. raciborskii* first appeared in the lake in 1979 and has a high and narrow optimum temperature range (22~24 ^oC) for germination of spores and its blooms are erratic and spike-like, indicative of a *P*-storage dependence similar to *Gleotrichia echinulata*. In the case of *G. echinulata,* phosphorus pools of freshly recruited colonies were estimated to be sufficient for 3 to 4 subsequent doublings, while *C. raciborskii* was reported to be able to store phosphorus adequate for two cell divisions (Shafik *et al.*, 1997). Any successful water-quality modeling effort involving these algal species, therefore, must address the *P*-storage dependence by applying a "variable cell-quota" concept in the phytoplankton dynamics.

Présing *et al.* (1996) found that, during the 1994 bloom, NH_4-uptake contributed to 85% of the *N*-demand in the *Siófok* basin and 50% in the *Keszthely* basin despite the ambient NH_4-*N* concentration being below 3 $\mu g/l$. The rest of the *N* requirement was furnished by N_2-fixation. This finding clearly indicates that *C. raciborskii* grows efficiently by assimilating NH_4-*N* as well as atmospheric nitrogen, and hence its blooms in the lake are not governed by *N*-limitation.

Experiment by Kovacs (1997) showed that *C. raciborskii* thrives well in a phosphorus-poor environment with low light intensity, dominating all competitors. According to Shapiro (1990), *C. raciborskii* is a typical cyanobacteria, whose dominance is promoted by a number of adaptations: higher temperature optima; low light requirement; vertical mobility in response to irradiation and nutrient supplies; ability to assimilate inorganic carbon at high *pH*; and not being grazed by zooplankton.

In view of the above accounts, the *JICA Study Team* has addressed phosphorus as the limiting nutrient in *Lake Balaton* water quality modeling.

With regard to the spatial distribution of water quality in the lake, the earlier *Balaton* studies have focused on the longitudinal distribution along the major axis of the lake by applying either multi-box type or one-dimensional modeling approaches. While this strategy can be justified in view of simplicity as well as the observed steep water quality gradients in the east-west direction, the two dimensionality of the phosphorous load into the lake is difficult to ignore. In terms of the external phosphorous load by all the rivers draining to the lake, *Zala River* contributes more than 50%. However, when the unevenly distributed loads along the shoreline are included, *Zala*'s contribution diminishes to mere 30%. This, along with the two-dimensionality of the wind-driven hydrodynamics in the lake, implies that the lateral variance of water quality could also be significant. On this rationale, the *Study Team* has committed to develop a fully two-dimensional water quality model for *Lake Balaton* to render both the lateral and longitudinal distributions of the water quality. To drive the mass transport process by the lake currents in the water quality model, a separate two-dimensional hydrodynamics model has also been developed.

Lake Balaton is also noted for its shallowness, averaging only 3.2 *m*, and remarkably low rate of through flow. In terms of water balance, the discharge by *Sio River*, the only outflow from the lake, is overshadowed by the evaporation loss and, therefore, the bottom sediments in the lake basin acts as a huge sink to the external nutrient loads. In this connection, Gelencser *et al.* (1982) estimated that the phosphorus retention in Lake Balaton can be as high as 95%. The commonly accepted notion that the detention time of the lake being about 2 *years* can be a misconception, from the perspective of water quality, since it was calculated by dividing the lake volume by all the water input combined including the precipitation, but disregarding the evaporation. In terms of water refresh cycle, the lake volume should be divided by outflow, which yields approximately 4.7 *years* for the detention time.

Although a very large proportion of the phosphorus accumulated in the sediment is apparently not biologically available for algal growth, it is the thin unconsolidated surface layer that plays a significant role as a source of internal load by re-suspension and diffusion processes. Istvánovics *et al.* (1989) reported that the phosphorus stored in the surface layer of the bottom sediment is about two orders of magnitude greater than in the overlying water.

As will be discussed in detail in a later section, this loose surface sediment layer is readily agitated by wind-driven currents and wave actions, and is easily re-suspended into the water column and re-settles under calm conditions. This mixing layer thickness is estimated to be about 10 *cm* (Lijklema *et al.*, 1983). Taking a conservative annual deposition rate of 3 *mm* (Lijklema, 1983; Herodek, 1989), this 10 *cm* of sediment surface layer represents at least 30 *years* of well-mixed "history", indicating that the biologically significant slice of the sediment has no "memory".

On this ground, the *Study Team* has resolved to exclude the sediment layer as an independent model compartment (state variable) and, instead, to focus on the sediment-water column interaction processes.

The wind-induced sediment re-suspension also affects the algal growth by light attenuation (*e.g.* Glenscser *et al.*, 1982; Luettich *et al.*, 1990). Somlyódy and Koncsos (1991) reported that light limiting conditions for algal growth frequently occur in Lake Balaton by wind-induced re-suspension. The *Study Team* has endeavored to incorporate the complexity of the sediment process in the biogeochemical model component.

One of the surmounting difficulties in developing any water quality model involving biogeochemical processes stems from the fact that algal dynamics are non-conservative, while nutrients are conservative substances. Taking into account also the fact that every shallow lake has its own characteristics, it is evident that development of a water-quality model applicable to all lakes is an unattainable goal. Often, the conceptual framework cannot be realized within the light of available information. Indeed, no existing model has proven to be successful in a general sense and the previous efforts to model the *Lake Balaton* water quality are no exception.

Notwithstanding, the *JICA Study Team* has striven to develop a robust model by taking known major biochemical processes into account and combining them with more deterministic sub-models for the physical processes. During the course of development and calibration, the *Study Team* also endeavored to utilize numbers and figures taken from actual measurements found in the previous *Lake Balaton* studies, as well as from field and laboratory studies undertaken by the present *JICA* program.

2. CONCEPTUAL STRUCTURE OF THE SIMULATION MODELS

The conceptual structure of the model developed for the present study is shown in *Figure C.4*. As a sub-component to the overall two-dimensional water quality model, a completely-mixed (0-dimensional) algal dynamics model, shown in *Figure C.5*, has been developed. Extensive parameter calibration and sensitivity studies have been undertaken using this sub-model referred to, here, as "*0-D WQSM*". Calibration results are discussed in *Section 4.1* of this *Appendix*.

The characteristics of the *Lake Balaton* hydrodynamics have been studied using a two-dimensional hydrodynamics model referred to as "*2-D HDSM*", incorporating local wind fetch and ground roughness effects using multi-station wind data as will be discussed in a later section. *2-D HDSM* has been calibrated and verified using multiple storm event data. A two-dimensional water-quality model called "*2-D WQSM*" has also been developed by combining a mass-transport model with the biogeochemical component. The mass transport sub-

model of *2-D WQSM* is driven by unsteady flow field generated by *2-D HDSM.* Upon satisfactory calibration and verification, all the sub-models: the hydrodynamics, the biogeochemistry, and the mass transport have been integrated to form a "*2-D Balaton Water Quality Model*" that has been utilized to investigate the impact of various nutrient loads and to assess the effects of eutrophication abatement strategies.

3. HYDRODYNAMICS SIMULATION PROGRAMS (2-D HDSM)

3.1 GOVERNING EQUATIONS

The governing equations for the hydrodynamics model consist of the unsteady nonlinear version of the depth-integrated shallow water equations, including convective acceleration, quadratic bottom friction, surface wind shear stress, and *Corioli's* effect. The wind stress incorporates the local fetch effect. The horizontal eddy viscosity terms are evaluated locally based on the Smagolinski's (1963) *LES* approach. The dependent variables are the x- and y-components of specific flow rates, and the surface elevation. The external forcing factors are the wind stresses and inflows and outflows. *Table C.1* shows the set of governing equations for the hydrodynamics component.

3.2 NUMERICAL METHOD

The computational scheme employs the Finite Element Method for its convenience in variable and arbitrary local resolution refinement as well as in detailed boundary-fitting capability. In addition, the scheme utilizes the "mass lumping" technique (see, for example, Segerlind, 1984) to eliminate matrix operations to achieve optimal computational efficiency. The spatial resolution is of order of 10- to 100-meter, utilizing 7199 triangular elements of variable size. The final FEM discretization of *Lake Balaton* is shown in *Figure C.6.* The mesh was generated by a mesh generator based on a strategy for near-constant *Courant Number* and was adjusted manually for local refinements. The mean water depth contours, drawn directly from the nodal depths of the elements, are shown in *Figure C.7.* Using a workstation equipped with a *DEC Alpha* 433 *Mhz* CPU, and the aforementioned 7119 elements, a real-time simulation for 4 *days* with a 20-*second* time step takes approximately 12 *minutes*, a respectable figure in terms of computational efficiency.

3.3 CALIBRATION AND VERIFICATION OF THE HYDRODYNAMICS MODEL

The influence of the wind overwhelms the slow hydrologic through flow (on the order of 1~2 *m/day*) in formation of the flow pattern in *Lake Balaton.* The shallowness of the lake results in fast response to winds, generating currents orders of magnitude greater than those produced by the through flow. The calibration and verification of any hydrodynamics model for *Lake Balaton* must

address to this nature.

Such processes have been fully incorporated into *2-D HDSM* using recorded storm events and wind data. Although the present hydrodynamics model involves only two adjustable parameters: the wind drag and the bottom roughness coefficients, some difficulties were encountered in interpreting available wind data. Wind data around the lake are sparse, at only four stations: *Keszthely*, *Siófok*, *Balatonakali*, and *Balatonszemes*.

The former two stations operated by the *National Meteorological Service* (*OMSZ*) provide hourly wind data with 1 *m/s* - 10^{o} resolution, averaged over 10 *minutes*, while the latter two operated by the *Central Transdanubian Water Authority* (*KDT-VIZIG*) unfortunately provide only 1.6 *m/s* - 45^{o} resolution, also averaged over 10 *minutes*. In addition, the hills along the northern shoreline of the lake are known to generate local effects by blocking and deflecting the prevailing winds from the *NW* quadrant, producing non-uniform wind field over the lake surface. *Keszthely* station, located approximately 1 *km* inland from the western bay shore, typically records significantly lighter winds than the other stations. During the in-lake field survey undertaken by the *Study Team* in 1997, there were occasions when the in-lake wind magnitude at the center of *Keszthely Bay* was measured at 4 *m/s* while the inland station, less than 4 *km* apart, recorded 0 *m/s* wind simultaneously.

Thus, using these raw wind data from the 4 stations to generate unsteady two-dimensional wind stress fields by spatial interpolation would not be a good representation of the reality. The *Keszthely* wind data unarguably need to be adjusted for the land to water roughness translation, as well as for the effect of wind fetch over the water surface since the prevailing wind is almost always from the *NW* quadrant. For this reason, the study team has resolved to apply adjustments to the *Keszthely* wind data following the procedure outlined by Cook (1985) for roughness change and fetch effect in which local in-lake wind speed is a function of down-wind distance from shoreline. The concept of effective fetch (*CERC*, 1974) is also applied to determine the fetch length. Since, the *Siófok* station is located right on the southern coast, downwind of the prevailing wind, such adjustments are deemed unnecessary. The wind data at *Balatonakali* and *Balatonszemes* were not utilized in the present study for their low directional resolution. Therefore, even with the adjustments, the sparsity of wind data would not be fully compensated for, and could be a considerable source of inaccuracies in modeling the lake hydrodynamics.

Figures C.8 to *C.11* show the calibrated results of the hydrodynamics model using wind data and water-level record taken during the storm event of March 31 to April 3, 1994. *Figure C.9* illustrates the effectiveness of the aforementioned wind speed correction procedure, and *Figures C.10* and *C.11* show the sensitivity of the model to the two adjustable parameters: the bottom roughness coefficient and the wind drag coefficient. Based on these results, the bottom roughness has

been optimized at n=0.02, and the Wu's (1973) wind drag coefficient as a function of wind speed has been selected for subsequent computations.

Three cases of the calibrated calculations for hindcasting the past storm events are shown in *Figures C.12 to C.19*. In the figures, the first case represents the storm event recorded by Muszkálay (1966) during the period July 8 to 9, 1963, and both the second and the third cases correspond to the events recorded by *VIZIG* during May 26 to 30, 1993 and March 31 to April 3, 1994. In the first case, only the *Keszthely* wind data were applied, in both the adjusted and unadjusted forms, as the *Siófok* data are not available. In the second and the third cases, the *Keszthely* wind data were adjusted according to the aforementioned manner, while the *Siófok* winds were unadjusted.

The event of July 8 and 9, 1963, the first case, driven by strong *WNW* winds, produced a wind setup and subsequent transverse seiche. Hindcasts for the water levels at *Balatonkenese* as well as for the discharge through *Tihany Straight* are generally satisfactory (*Figure C.12*) while the water levels at *Keszthely* are less satisfactorily reproduced, presumably resulting from the inadequacy in wind data, both in terms of the density of recording stations as well as the temporal resolution.

Missing from the model result for the water elevation are the high frequency oscillations found in the observation record caused by transverse seiche. Most likely, this is attributable to the filtered wind record (10-*minute*-averaged hourly values) as compared to approximately the 40-*minute* transverse seiche period. *Figures C.13* and *C.14* show the computed water level contours and flow field at 17:30 July 8, 1963 during the same storm event. Since the wind direction is nearly perpendicular to the longitudinal axis of the lake, the wind setup occurred only in the transverse direction. The flow pattern, on the other hand, shows complex gyre formations.

Both of the two storm events of May 26 to 29, 1993 (*Figures C.15* to *C.17*) and March 31 to April 3, 1994 (*Figures C.9, C.18,* and *C.19*) represent the cases of longitudinal wind forcing. Both the cases generated significant longitudinal setup and seiche as expected. Hindcasts for the water elevations at the four stations: *Tihany*, *Balatonaliga*, *Balatonakali*, and *Keszthely*, are quite satisfactory (*Figures C.9* and *C.18*), indicating that the calibration procedure has been successful. The short-period oscillations conspicuous at around time=72 *h* seen in *Figure C.9* for the March-April 1994 event are likely the transverse seiche resulting from the sudden shift in the wind direction at time=48 *h*.

Figures C.16 to *C.19* show the computed water level contours and flow fields during the corresponding two storm events. As the direction of the strong winds coincide with the longitudinal axis of the lake in both the cases, current vectors are nearly uniformly pointed to *Siófok Bay* except at the very end of the bay where a weak clockwise gyre is formed. Expectedly, the corresponding water

level contours are nearly perpendicular to the longitudinal axis, showing typical wind setup phenomena.

3.4 DEVELOPMENT OF A PARTICLE TRACKING PROGRAM

As an analytical tool for assessing the mixing process in the lake, a particle tracking procedure has been developed. The procedure is based on a *Lagrangean* linear vector addition computed at each of the hydrodynamic time step. "Particle", here, signifies a flagged (marked) water particle with the same properties with the ambient.

Figures C.20 and *C.21* are visualization of the annual mixing processes for 1994 and '95. In the figures, the multi-colored particles are placed in the four basins, *I* to *IV*, as the lake has been customarily divided, at time=0:00 *h*, January 1st of the respective year, and their subsequent movements by the storm were traced for 365 *days*. Some particle losses, resulting from the mixed *Euler-Lagrange* scheme, are unavoidable. Nonetheless, it can be seen that the degree and the pattern of annual mixing are similar for 1994 and '95. Since 1994 was noted for the algal bloom of unprecedented scale while 1995 experienced no bloom, it is evident that the difference in mixing pattern is not a significant factor related to the occurrence of the extraordinary algal growth.

Figures C.22, and *C.23* are results of particle tracking for *Zala River* and *Nyugati River* discharge for 1994 and '95. In the calculation, particles were released at intervals reflecting the flow rate of each river, and their subsequent trajectories were traced. It is seen that the river water traveled longer distance in 1995 than in 1994. It is noteworthy that the *Keszthely Basin* is well mixed even at the early stage of a year.

4. WATER QUALITY MODEL

4.1 COMPLETELY-MIXED BIOGEOCHEMICAL MODEL (0-D WQSM)

(1) Previous Models

Three types of previous model exist for investigation of the phytoplankton dynamics of *Lake Balaton*: *BEM*, *BALSECT*, and *SIMBAL*. The characteristics of these models were reviewed by van Straten and Somlyódy (1980), and are summarized as follows:

The *BEM* model is the earliest developed by the *Hungarian Balaton Ecological Modelers Group* (Kutas and Herodek, 1982). Emphasis of the model is placed on description of the phytoplankton biomass and the daily primary production. The model *BALSECT* (Balaton Sector Model) was developed at *IIASA* based on an earlier more general phosphorus and nitrogen cycle model. It concentrates

on the analysis of phosphorus compound transformation in the lake (Leonov, 1980). The *SIMBAL* model (Simplified Balaton Model), the most extensively studied model among the three, consists of a set of models designed especially to investigate various hypotheses regarding the modes of phosphorus interaction between the water and the sediment (van Straten, 1980). The conceptual structures of the three models are illustrated in *Figure C.24.*

van Straten (1980) addressed the uncertainties in data utilized in his calculation of the *SIMBAL* by presenting a probability distribution around the mean time trajectory. In the calculation, the lake was divided into four basins assuming a constant hydrological exchange rate between the neighboring basins. Comparison between the calculations and measurements were made for the four basins of the lake only during a year of 1977 as seen in *Figure C.25.* In addition, the distribution of the nutrient loads over the months of the year was simply based on an assumption. These shortcomings were recognized, and van Straten and Somlyódy (1980) subsequently suggested multi-year calibrations and improvements on the nutrient load conditions as subjects of future study. In the model output, the bimodal peaks of phytoplankton phosphorus during the spring and summer seasons were satisfactorily reproduced, although the summer peak in *Keszthely Bay* was considerably lower than the measurement as seen in the figure.

Luettich and Harleman (1986) introduced a variable cell-quota concept into *SIMBAL* to improve the model performance (see also Baker, 1982). The model was applied only for the period between June and December, 1977 for the *Keszthely* basin. The calculated *Chla* concentrations compare favorably with the measurements, while PO_4-P concentrations remained below 1 mg/m^3 during the growth period with some increase later in the year, an intuitively reasonable outcome. van Straten (1980) found that the early version of *SIMBAL* which excluded a bulk transfer process with the sediment gave unreasonable phosphate levels late in the year. He considered this finding as a necessity to include the exchange process in his final *SIMBAL* model. On the other hand, Luettich and Harleman (1986) obtained relatively reasonable results with a reduced bulk exchange coefficient, and suggested its insignificance in the overall process. However, two sets of numerical experiments without the bulk transfer showed conflicting results, and they attributed this difficulty to the insufficiency in the exchange modeling due primarily to the inability of calibration with the given data set.

In both the cases, the calculations were carried out using only a single-year data set, so that it is difficult to deduce an appropriate model system based only on these studies. Furthermore, the sediment-water interaction was only included as a bulk diffusion process, and the phosphorus adsorption/desorption processes associated with the wind-induced sediment resuspension was not incorporated.

Leonov (1985) applied *BALSECT* to simulate a relatively long-term phosphorus

cycle in the four basins of *Lake Balaton* during 1976~1979. Computed results are within a range comparable to the measured values; however, disparities in phase and annual maximums are substantial.

BALASECT consists of five state variables, of which dissolved organic-*P* and bacterial-*P* are difficult, if not impossible, to analyze and to establish rate-constants. In addition, data for directly measured phosphorus fractions, necessary for the model calibration, such as total dissolved phosphorus, particulate inorganic, and phytoplankton-*P* are not readily available for investigation.

Kutas and Herodek (1986) applied *BEM* to the four basins of *Lake Balaton* to reproduce *Chla* concentrations in 1976 and 1977. The composition of algal species during that time was more complex than that in the '90s, so that four different types of algae were dealt with in the calculation. However, the hindcasts of the peak values of *Chla* during the summer in the *Keszthely* and the *Szigliget* basins were not satisfactory. The calculated maximum was lower in 1976 and was significantly higher in 1977 than measurements.

(2) Framework of the Biogeochemical Model

Since the growth of heterocytic cyanobacteria such as *C. raciborskii* is not limited by nitrogen, the biogeochemical component of the water-quality model in the present study is also a phosphorus cycle model as found in the previous models. Despite the considerable uncertainties in clarifying the process of sediment-water interaction of phosphorus, the *Study Team* has resolved to include such processes. Some of the evidences such as those found by Gelencser *et al.* (1982) and Istvánovics *et al.* (1989) that the rate of *P*-desorption from the sediment resuspended by even a moderate storm could be comparable in magnitude to the daily average external load, and that high algal growth rates were observed in incubation with the lake sediment (Dobolyi and Ördög, 1997), strongly suggest the importance of the sediment processes on the algal growth.

The developed model consists of four variable components: orthophosphate (*PO_4-P*), phytoplankton-*P*, detrital-*P* and algal dry-weight biomass plus the suspended sediment concentration that relates to the *P*-sorption processes and the light transmission. Bottom sediment layer, *per se*, is not included as an independent variable (compartment) since the mobile bottom layer, representing at least decades of accumulation, is well mixed and has no memory. Instead, emphasis is placed on addressing the bulk diffusion process from the bottom sediment, as well as the effect of wind-induced sediment re-suspension both in terms of the *P*-exchange with the water column and the light attenuation. The underlying strategy, here, is to minimize uncertainties while utilizing known and proven processes supported by data to a full extent. Unlike the previous model studies, most of the model parameters used in the present study are based on existing database specifically for *Lake Balaton* substantiated by field and laboratory studies conducted during the past decades.

Within a water column, phosphorous removal is primarily due to the uptake by phytoplankton, and contribution by biogenic lime co-precipitation or adsorption by suspended sediment is negligible (Herodek, 1986). The present modeling strategy also follows this finding. As discussed earlier, a variable cell-quota sub-model is incorporated addressing the phosphorus storage ability of blue-greens such as *C. raciborskii*. The suspended sediment (*SS*) concentration is dynamically calculated simultaneously with the four independent variables. The rate of phosphorus desorption from the sediment is modeled as a function of *SS* concentration. The conceptual structure of the sub-model is referred to *Figure C.5*, and its governing equations are shown in *Table C.2*. The characteristics of the sub-models are described below:

1) Phytoplankton dynamics

Since *C. raciborskii* is the predominant specie in *Lake Balaton* as stated previously, its growth characteristics are considered representative of the phytoplankton growth in the lake water. A laboratory experiment conducted by *KDT-KÖFE* (1988) using *C. raciborskii* isolated from *Lake Balaton* and cultured in *Allen-N* medium found that the maximum growth rate was 0.96 day^{-1} at an optimum temperature of 23 ^oC as shown in *Figure C.26*. On the other hand, an experiment by Shafik *et al.* (1987), in which *C. raciborskii* was cultured with different nitrogen sources: N_2, NO_3, and NH_4, exhibited a higher maximum growth rate of 1.7 day^{-1} at a higher optimum temperature of 30 ^oC as seen in *Figure C.27*. Since the water temperature in the *Keszthely* basin surpassed 30 ^oC when a large bloom of *C. raciborskii* occurred in 1994 and there is apparently a good correlation between the air temperature and occurrence of bloom (Kóbor, 1997; Padisák and Istvánovics, 1996), the latter experimental data are adopted in the current model. The overall growth rate is formulated by multiplying the maximum growth rate by limiting functions of internal nutrient, temperature, and light. The characteristics of the functions are described below:

a. Nutrient limitation

Although nitrogen is not a limiting nutrient for heterocytic cyanobacteria, its growth rate varies depending on the available form of nitrogen as seen in *Figure C.27*. *C. raciborskii* appears to utilize atmospheric nitrogen only after NH_4 and NO_3 are depleted. Cyanobacteria are apparently able to assimilate ammonium at very low ambient concentration. During the 1994 bloom, ammonium utilization contributed to 80 % of the nitrogen uptake in the *Siófok* basin, while it was 44 % in the *Keszthely* basin. In the latter case, regeneration of NH_4 within the basin was insufficient to sustain the very large algal population so that N_2 fixation played more important role than the former case contributing to nearly 50 % of the nitrogen uptake (Présing *et al.*, 1996). While the maximum growth rate varies as much as 30 % depending on the forms of nitrogen source, the rate compatible with NH_4 has been adopted in the present study, as it is the first to be assimilated by *C.*

raciborskii.

The growth limiting factor for nutrients is formulated as a function of the internal level of PO_4-P in the algal cell. The internal concentration is defined as a "cell quota," i.e., ψ = (internal mass of phosphorus in cells)/(dry weight biomass of cells). The internal nutrient level depends on the relative magnitude of the nutrient uptake rate and the algal growth rate. The uptake rate is a function of both the internal and the external nutrient concentrations, while the growth rate depends primarily on the internal concentration. A *Monod* type equation is used to calculate the external uptake rate, and an equation of Droop (1973) is used as the internal nutrient limitation.

An experiment by Shafik *et al.* (1997) showed that ψ_{max} and ψ_{min} of *C. raciborskii* are 1.4% and 0.32%, respectively. The ψ_{max} value corresponds to the *P*-storage capacity sufficient for two subsequent cell divisions in the absence of external *P* source. These values were somewhat modified in the calibration process, and were settled at ψ_{max} =1.8 % and ψ_{min}=0.2% . The characteristics of the cell-quota functions are shown in *Figure C.28* corresponding to these values. It is seen that the value of $f(\psi)$ decreases rapidly when the algal phosphorus content becomes less than 30% of the maximum capacity. On the other hand, the cell quota function, $f_N(\psi)$ for algal nutrient uptake decreases linearly with the algal phosphorus content.

b. Temperature limitation

As discussed previously, the optimum growth temperature for *C. raciborskii* has been chosen at 30 ^oC. The growth rates measured by Shafik *et al.* (1997) are normalized by the maximum growth rate. The obtained curve fits well to the temperature limiting function formulated by Lerman *et al.* (1975), as shown in *Figure C.29*, by selecting the optimum, and the upper and lower limits at 30, 40, and 18 ^oC, respectively.

c. Light limitation

A laboratory experiment found that the growth of *C. racborskii* is not inhibited by strong light intensities, indicating that a saturation type of light limiting growth function is needed (*KDT-KÖVIZIG*, 1988). The *Steele's* light limiting equation is, therefore, modified to a non-inhibiting function as shown in *Table C.3*. The function *f(I)* is integrated over the depth for use in the *0-D* and *2-D* models (*Table C.3*). The magnitude of the integrated function, $\bar{f}(I)$, is quite sensitive to the light extinction coefficient K_e. Taking the average depth of 2 *m* in the *Keszthely* basin, and using K_e=1.0 and 3.0 m^{-1}, a commonly observed range, $\bar{f}(I)$ value with K_e =1.0 becomes more than twice that with the latter K_e (see *Figure C.30*). This exemplifies the model sensitivity to the extinction coefficient.

Since algal growth can also be limited by the light attenuation, resulting from

the wind-induced sediment re-suspension in *Lake Balaton*, the extinction coefficient needs to be modeled as a function of *SS* concentration. Somlyódy and Koncsos (1991) proposed a reduced form of equation to calculate the extinction coefficient as a function of wind speed. The calculated time-series of extinction coefficients agreed well with measured values in the *Siófok* basin, where the influence of algal biomass on the coefficient is presumably negligible. Since *SS* concentration can be calculated by using physically more straightforward manner, i.e. based on the bottom shear stress, the present study, as will be described later, has opted to correlate extinction coefficients with the concentrations of *SS* directly.

Since no previous formulations are available to correlate the extinction coefficient to *SS* and *Chla* combined, existing field data as well as data collected during a field study program of the present project are applied. During the field study, vertical light quanta were measured at every 50 *cm* depth in June, July, and August 1997 at several locations in the entire lake basin. A local extinction coefficient, K_e, at each station was calculated based on *Lambert-Beer's law*. Correlation between the calculated and the measured value is high, with better than r=0.98. Since *Chla* concentrations during the survey were relatively low at less than 20 mg/m^3, contribution of *Chla*-induced extinction coefficient, $K_{e,Chla}$, may be subtracted from total coefficient, K_e, without introducing significant errors, by using a simple relationship: $K_{e,\ Chla}\ [m^{-1}] = 0.02\ Chla\ [mg/m^3]$ (Matsuoka, 1984) with $K_e = K_{e,\ Chla} + K_{e,\ SS}$. This procedure yields an equation of *SS* -induced extinction coefficient, $K_{e,\ SS}$, as shown in *Figure C.31*.

Next step is to derive an equation of $K_{e,\ Chla}$ for a wider range of *Chla*. Data taken by *KDT-KÖFE* for *Chla, SS* and *secchi* depth during June and October of 1984~1996 are utilized for this process. First, the *secchi* depth is correlated with K_e by selecting data for $Chla < 20\ mg/m^3$ and $SS < 50\ mg/m^3$ where K_e is the sum of $K_{e,\ Chla}$ and $K_{e,\ SS}$ as assumed in the previous step. Second, another data set for $Chla > 50\ mg/m^3$ and $SS < 50\ mg/m^3$ is assembled from the data pool to derive a correlation for $K_{e,Chla}$, as shown in *Figure C.33*. Although the data points scatter considerably with r=0.7, $K_{e,Chla}$ for higher concentrations of *Chla* can be estimated by the equation. Combining both the equations, the total extinction coefficient can be expressed as $K_e\ [m^{-1}] = 0.2 + 0.059\ SS\ [g/m^3] + 0.019\ Chla\ [mg/m^3]$. The second factor for *SS* contribution is similar to that of Di Toro (1978) and the third factor for *Chla* is comparable to that of Matsuoka (1984).

2) Suspended sediment modeling

The sediment of the lake primarily consist of fine silt and clay except near the southern shore and in *Tihany Strait* where coarser fractions prevail. Suspended sediment concentrations in the lake are calculated using the method by Luettich *et al.* (1990) as shown in *Table C.4*. The stress by the mean current is

disregarded by comparison to the stress by the wind-induced wave actions. Wave heights utilized for the suspended sediment sub-model are evaluated using the shallow-water modifications to the *SMB* method presented by *CERC* (1974) as shown also in *Table C.4.* The predicted wave heights as well as *SS* concentrations in *Keszthely Bay* are in good agreements with the measurements by Luettich *et al.* (1990), as displayed in *Figures C.34* and *C.35*, in which the best fitting parameters differ somewhat from those used by Luettich *et al.* (1990).

This sub-model is applied to hindcast the *SS* concentrations at the center of *Keszthely Bay* in 1992 by using hourly wind data measured at the *Keszthely* weather station. The calculation reproduced relatively well the values measured by *KDT-KÖFE* as seen in *Figure C.36.* Although the minimum *SS* concentration of 15 *mg/l* was suggested by Luettich *et al.* (1990), measurements undertaken by *JICA Study Team* yielded a lower value at 5 mg/m^3. The latter value is used as the background concentration in the present study.

3) External nutrient loads modeling

The loads from *Zala River*, direct runoff, and atmospheric deposition are considered in the 0-D model calculation as the external loads to *Keszthely Bay.* Daily measurement data for PO_4-*P*, Total-*P* (*TP*), and *Chla* are available for *Zala River.* Annual *TP* load by the direct runoff, estimated in the earlier chapter, is converted into daily load in proportion to the precipitation in the area. Contribution of PO_4-*P* in *TP* is determined by measurements during the present study. Atmospheric deposition data are assembled by using measurements for PO_4-*P* and *TP* (*Hidrological Kozlony*, 1973) and daily precipitation (*OMSZ*).

A point of notice is the drastic change in water quality of *Zala River* after the completion of the second *Kis-Balaton* reservoir in 1993. Annual average PO_4-*P* concentrations of the river water jumped from 20~30 $\mu g/l$ during the years 1990~1993 to 90~100 $\mu g/l$ during the period 1994~1995 as seen in *Figure C.3.*

4) Internal nutrient loads modeling

As the major internal nutrient loads generated by the sediment-water interaction, bulk diffusion and sorption processes are incorporated in the current modeling framework.

a. Sediment characteristics

The mixing layer thickness of the bottom sediment by wave-motion and currents is about 10 *cm* (Lijklema et al., 1983). Since annual maximum sediment deposition rate is about a few mm (Lijklema, 1983; Herodek, 1989), time required for the deposition of the mixed layer can be estimated being at least 33 *years* as shown in *Figure C.37.*

Another estimate by taking an average *TP* contents in the sediment of 0.8 *mg-P/g-dry sediment* with a density of the dry sediment = 2.6 g/cm^3; with 11 % dry sediment per unit volume; and *TP* load of 1.2 $g/m^2/year$, yields an accumulation time of about 20 *years* for the 10 *cm* surface layer.

Sediment core data also support the estimate for the mixing layer thickness. *Table C.5* shows average phosphorus concentrations of 11 sediment cores taken along *Lake Balaton* in 1978 and 1995 (Dobolyi, 1995). It can be seen that extractable phosphorous (*EP*) components as well as *TP* distributions are nearly uniform in the top 10-*cm* layer of the sediment cores. The differences of total-*EP* and *TP* concentrations between the 0 ~ 5 and the 5 ~10 *cm* layers are less than *5 %*.

Even sediment core samples taken in the area 20 ~ 100 *m* offshore in the northern *Keszthely Bay*, where the bottom disturbance is expected to be minimal owing to the shortest fetch in the prevailing wind direction, exhibit small vertical variance in phosphorous concentration. Average *TP* of 49 samples in 0~10 *cm* and 10~20 *cm* layers differ only 8 %, at 755 and 696 *mg-P/g-dry sediment*, respectively (*BVK, Balaton Branch Office*, 1992). Average of 23 samples taken in the same area by *KDT-VIZIG* in 1994 shows only 5 % difference: 533 and 505 *mg-TP/g-dry sediment*, in 0~10 and 10~20 *cm* layers (*KDT-VIZIG Report,* 1994).

As estimated earlier, the upper 20 *cm* of the bottom sediment layer represent about 40 to 70 *years* of well-mixed deposition. The "history" of the accumulated sediment, therefore, has no temporal resolution for a shorter time span. Since the current modeling is targeted for prediction of annual *Chla* levels in the lake, the past account of sediment has no relevance.

b. Diffusion process

Since more than 95% of total dissolved phosphorus released from intact sediment cores is in the form of PO_4-*P* (Istvánovics 1988), only PO_4-*P* release is considered in the diffusion process. The release of phosphorus from intact sediment cores taken at the center of the four basins in August 1997 were measured at 0.9~2.8 $mg\text{-}P/m^2/day$ on the third day of incubation (*JICA Study Team,* 1997). The values are very similar to those measured after 2~4 *days* of incubation by Istvánovics (1988) whose results varied seasonally between -0.5 and 2.8 $mg/m^2/d$, the latter maximum observed during the summer. Another set of experiments by Istvánovics (1988) showed a higher release rate of 4 $mg\text{-}P/m^2/day$ corresponding to the maximum *pH* value of 9.2 during the summer. A different approach by Lijklema *et al.* (1986) using a diffusion coefficient of 10^{-9} m^2 /*s* with mixing-layer thickness, $\delta_z = 2\text{x}10^{-2} \sim 2\text{x}10^{-3}$ *m*, and an interstitial PO_4-*P* concentration in a range of 50~250 mg/m^3 yields release rates of 0.2~10 $mg\text{-}P/m^2/day$.

A first order bulk-diffusion equation has been adopted in the current model as shown in *Table C.2*. Since the rate of phosphorus release is greater during the summer season, an equilibrium concentration of PO_4-*P* in the sediments is modeled using an interstitial PO_4-*P* level multiplied by a temperature correction factor. Considering also that laboratory-measured rates frequently underestimate *in situ* rates (Andersen, 1974; Ryding and Forsberg, 1977; Bostrom, 1982) the exchange rate has been chosen to fit within the range found by Lijklema *et al.* (1986). With the parameters listed in *Table C.6*, the release rate for a water temperature range, 5~25 ^oC, varies from 0.3 to 10 *mg-P/m*^{3}. There still is a room for further study in the estimation of phosphorus release rates to narrow down the uncertainties in the laboratory values.

c. Sorption process

The rate of adsorption of phosphorus by *calcite*-rich sediments in Lake Balaton is slow, taking 7 to10 *hours* to attain equilibrium. (Gelencser *et al.*, 1982, Istvánovics *et al.*, 1989). On the other hand, desorption process completes within 30 *minutes*. A threshold concentration, at which neither adsorption nor desorption takes place, determined from *Langmuir* isotherm is in the range of 10 to 18.1 *μg/l* (Istvánovics *et al.*, 1989). Since PO_4-*P* level in the lake water seldom exceeds 10 *μg/l* (Presing *et al.*, 1996), only the desorption process is considered in the present model.

Phosphorus liberated from the re-suspended sediment through the desorption process was calculated based on an experiment by Gelencser *et al.* (1982). In the experiment, increase in PO_4-*P* concentration was measured in triplicate with the same sediment samples using lake water, without addition of phosphorus but with *SS* concentrations in a range of 70 to 1300 *g/m*^{3}, allowing a reaction time of 30 *minutes*. The PO_4-*P* increase per unit dry material of *SS* (=*DM*), $\Delta C/SS$, varied 5~15 *μg-P/g-DM* as shown in *Figure C.38*. The desorption rates, $\Delta C/SS$, corresponding to *SS* concentrations less than 180 *mg/m*^{3}, the maximum *SS* concentration in the lake (unpublished data by Dobolyi, 1997), are plotted in *Figure C.39*. However, the large scatter arising from uncertainties in the laboratory analysis does not allow establishment of a $\Delta C/SS = f(C_e)$ relationship in a straightforward manner. $f(C_e)$ was, therefore, presumed as a constant in the present study at 10 *μg-P/g-DM*, the average value taken from the figure.

Figure C.40 shows a comparison of PO_4-*P* load from *Zala River* with the *SS*-induced internal load in the *Keszthely* basin during 1994, in a cumulative form. It can be seen in the figure that the *SS* contribution of PO_4-*P* amounts to about 60 % of the *Zala* load, exemplifying the significance of the internal load in *Lake Balaton*.